



HAL
open science

Early Triassic chondrichthyans from the Zuodeng Section, Guangxi Province, South China: Palaeobiological and palaeobiogeographical implications

Jiachun Li, Zuoyu Sun, Gilles Cuny, Dayong Jiang

► **To cite this version:**

Jiachun Li, Zuoyu Sun, Gilles Cuny, Dayong Jiang. Early Triassic chondrichthyans from the Zuodeng Section, Guangxi Province, South China: Palaeobiological and palaeobiogeographical implications. *Palaeogeography, Palaeoclimatology, Palaeoecology*, 2023, 624, pp.111635. 10.1016/j.palaeo.2023.111635 . hal-04116998

HAL Id: hal-04116998

<https://hal.science/hal-04116998>

Submitted on 5 Jun 2023

HAL is a multi-disciplinary open access archive for the deposit and dissemination of scientific research documents, whether they are published or not. The documents may come from teaching and research institutions in France or abroad, or from public or private research centers.

L'archive ouverte pluridisciplinaire **HAL**, est destinée au dépôt et à la diffusion de documents scientifiques de niveau recherche, publiés ou non, émanant des établissements d'enseignement et de recherche français ou étrangers, des laboratoires publics ou privés.

23 **Keywords:** Elasmobranchs; palaeobiodiversity; palaeobiogeography; Tethys; China.

24 1. Introduction

25 The end-Permian mass extinction (EPME), the most severe crisis of the Phanerozoic (Erwin, 1993;
26 Stanley, 2016; Fan et al., 2020), led to the turnover between Palaeozoic and Modern faunas (Sepkoski,
27 1981). Chondrichthyans, being one of the predominant top predators of the Late Palaeozoic marine
28 ecosystems (Pitrat, 1973; Chen and Benton, 2012; Koot, 2013; Romano et al., 2016), also experienced
29 a sharp turnover in the wake of the EPME when marine Palaeozoic stem chondrichthyans (e.g.,
30 cladodontomorphs, Petalodontiformes, Bransonelliformes) went extinct or strongly declined, whereas
31 the Hybodontiformes increasingly dominated and the modern sharks (Neoselachii) emerged in
32 Mesozoic marine ecosystems (Guinot et al., 2013; Manzanares et al., 2020). Thereafter,
33 chondrichthyans were one of the major vertebrates occupying higher trophic levels in Early Triassic
34 marine ecosystems so that relevant researches are crucial to understand chondrichthyan faunal
35 turnovers and ecosystem recovery after the EPME (Koot, 2013; Scheyer et al., 2014). Early Triassic
36 chondrichthyans have so far been reported from western United States (Mutter and Rieber, 2005),
37 western Canada (Mutter and Neuman, 2006, 2008, 2009; Mutter et al., 2007, 2008), Spitsbergen
38 (Stensiö, 1918, 1921; Birkenmajer and Jerzmańska, 1979; Błażejowski, 2004; Romano and Brinkmann,
39 2010; Bratvold et al., 2018), Greenland (Nielsen, 1952), Azerbaijan (Obruchev, 1965; Kasumzadeh,
40 2000), Turkey (Thies, 1982), Oman (Koot et al., 2015), Madagascar (Thomson, 1982), Japan (Goto,
41 1994; Goto et al., 1996, 2010; Kato, et al., 1995; Yamagishi, 2004, 2006), South Primorye Russia
42 (Yamagishi, 2006, 2009), Timor (Yamagishi, 2006) and South China (Dingri in Tibet: Zhang, 1976;
43 Zuodeng in Guangxi Province: Wang et al., 2001). The material from China is, however, insufficiently
44 described: a species of helicoprionid shark, *Sinohelicoprion qomolangma* was erected based on a

45 partial tooth spiral dentary with six teeth and a preorbital part of skull from South Tibet (Zhang, 1976)
46 and three poorly diagnosed shark taxa, '*Hybodus*' *zuodengensis*, '*Hybodus*' *yohi* and '*Polyacrodus*'
47 *tiandongensis*, were described based on six teeth from Luolou Formation at the Zuodeng section,
48 Guangxi Province, South China (Wang et al., 2001). The aim of the current study is 1) to present a
49 detailed study of a diverse chondrichthyan fauna from the Early Triassic of Zuodeng based on new
50 materials collected by bulk sampling; 2) to reconstruct the shark palaeocommunity in the region and its
51 palaeobiodiversity.

52 **2. Geological setting**

53 Geographically, the fossil locality (106°59'36"E, 23°27'12"N) is approximately 4.5 km southwest to
54 Denggao village, Zuodeng Town, Tiandong County, Guangxi Province, South China (Fig. 1A). The
55 Nanpanjiang Basin was made of deep-water sediments within which a number of isolated shallow
56 carbonate platforms, such as the Great bank of Guizhou (GBG), the Jinxi, Chongzuo, Debao and
57 Pingguo Platforms were scattered to form an archipelagic sea (Lehrmann et al., 2003, 2015; Enos et al.,
58 2006). The Zuodeng section was located between the Debao and Pingguo Platforms within the southern
59 (interior) part of the Nanpanjiang Basin (Fig. 1B).

60 Zhao (1959) first measured the Early Triassic Luolou Formation at the Zuodeng section and reported
61 on ammonoids therein. Yang et al. (1984) subdivided the Luolou Formation into twelve layers, where a
62 successive eight conodont zones were established (Fig. 2A). Subsequently, Wang et al. (2001)
63 described three elasmobranch species that were recovered from Yang et al.'s (1984) conodont residues,
64 i.e. '*Hybodus*' *zuodengensis*, '*Hybodus*' *yohi* and '*Polyacrodus*' *tiandongensis*, all from the conodont
65 *Triassopathodus homeri*-*Neospathodus triangularis* Zone (Fig. 2A). More recently, Yan (2013)
66 reassessed the Zuodeng section of Yang et al. (1984) and divided it into the Zuodeng I (ZD I) and the

67 Zuodeng II (ZD II) sections (Figs. 2B, C). Six conodont zones ranging from the early Induan to late
68 Olenekian were recognized on the ZD I section (Fig. 2B), whereas seven conodont zones ranging from
69 late Induan to late Olenekian were recovered on the ZD II section (Fig. 2C). Accordingly, the
70 Smithian-Spathian boundary between ZD I and ZD II is marked by the first occurrence of
71 *Icriospathodus collinsoni* on the ZD I and *Novispathodus pingdingshanensis* on the ZD II (Yan, 2013).
72 The present shark samples were collected from the upper part of the Luolou Formation, characterized
73 by an alternance of thin and thick bedded muddy limestone with shale, mudstone, marl and pisolitic
74 limestone interbeds (Fig. 1C, D). Their lithological and biostratigraphical correlations are illustrated in
75 Figure 2.

76 3. Material and methods

77 A total of 63 conodont samples (each weighting 5~10 kg and sampled at ~1 m intervals) and an
78 additional 10 bulk samples (each weighting about 25 kg) were collected in order to search for
79 shark-teeth-bearing layers in 2018. Then, 15 bulk samples (each ca. 25 kg) targeting for shark teeth,
80 were exclusively collected from the shark-teeth-bearing layers in 2020. After breaking coarsely the
81 samples into $\sim 2 \times 2$ cm pieces, they were dissolved in 10% acetic acid, and then filtered through 74 μm
82 and 2 mm meshes. All microfossils, including conodonts and shark remains, were handpicked using
83 fine writing brushes under a binocular microscope. A total of 55 shark teeth and 10 dermal denticles
84 were recovered. Shark teeth were photographed using a JEOL JCM-6000 Plus scanning electron
85 microscope (SEM) under an acceleration voltage of 10 kV. Six broken teeth were used for enameloid
86 analysis following the protocol described by Cuny et al. (2001). The material was etched with 10%
87 HCl for 5-30 seconds according to the size and type of the studied structure, and then was rinsed in
88 demineralized water for 10 minutes. Photographs of the enameloid structures were taken using a FEI

89 QUANTA-650FEG SEM with an acceleration voltage of 10 kV. The systematic framework and shark
90 tooth terminology follow Cappetta (2012) and Enault et al. (2015). The microstructural terminology
91 follows Cuny et al. (2001). The use of open nomenclature follows Bengtson's (1988) recommendations.
92 The quantitative analysis of the shark community was evaluated by the Simpson's Index (Simpson,
93 1949), Shannon Index (Shannon, 1948) and Evenness (Pielou, 1966) according to the following
94 mathematical formulas:

95
$$^{(1)} \text{Simpson's Index } (D) = \sum (n_i/N)^2$$

96
$$^{(2)} \text{Shannon Index } (H) = -\sum (P_i) (\ln P_i)$$

97
$$^{(3)} \text{Evenness } (E) = H / H_{\max} = -\sum (P_i) (\ln P_i) / \ln(S)$$

98 with N, the number of all teeth of a community; n, the number of teeth of a given species of a
99 community; P_i, n_i/N for each of the recovered species; S, the number of species of a community.

100 This study was conducted at the Laboratory of Orogenic Belt and Crustal Evolution, School of Earth
101 and Space Sciences, Peking University, China. All specimens are stored in the collections of GMPKU
102 (Geological Museum of Peking University, Beijing, China).

103 **4. Systematic palaeontology**

104 **(by J.C. Li and G. Cuny)**

105 Class CHONDRICHTHYES Huxley, 1880

106 Subclass ELASMOBRANCHII Bonaparte, 1838

107 Cohort EUSELACHII Hay, 1902

108 Order HYBODONTIFORMES Patterson, 1966

109 Family incertae sedis

110 Genus *OMANOSELACHE* Koot, Cuny, Tintori and Twitchett, 2013

111

OMANOSELACHE HALLI Koot and Cuny in Koot et al., 2015

112

(Figure 3A-C')

113

2006 *Lissodus* sp. 1 Yamagishi, pp. 79, pl. 5, figs. B-D.

114

Material—Sixteen teeth, GMPKU-P-3750-61, GMPKU-P-3788-91 and GMPKU-P-3799, from layers

115

8-11 of the Luolou Formation, Zuodeng section. Five specimens were used for imaging:

116

GMPKU-P-3750-54 and two for SEM microstructural study: GMPKU-P-3790 and GMPKU-P-3799.

117

Description—The teeth are elongate and fusiform in shape, measuring 0.9-2.3 mm mesiodistally,

118

0.3-1.0 mm labiolingually and 0.3-1.0 mm apico-basally. The dentition shows a gradient monognathic

119

heterodonty: anterolateral teeth have a strong main cusp and basally arched root, whereas the

120

posterolateral teeth have a weak main cusp and straight root. The crown is symmetric or asymmetric

121

with one prominent main cusp surrounded by several small lateral cusplets. In apical view, the mesial

122

extremity of asymmetric teeth (e.g. GMPKU-P-3752, GMPKU-P-3753) turns labially or lingually (Figs

123

3M, R). The main cusp is pyramidal in shape with a blunt apex. It always displays an overhanging peg

124

that is apicobasally extensive on the lingual face, whereas the corresponding peg on the labial face is

125

less developed (Fig. 3G) or absent (Fig. 3Q) or replaced by a concave depression (Fig. 3L). The lateral

126

cusplets are reduced and nearly fused together in most specimens (Figs. 3A, K, U). They vary in

127

number. For example, an anterolateral tooth (GMPKU-P-3751) shows five pairs of lateral cusplets on

128

the mesial and distal sides (Figs. 3F-J), whereas a lateral tooth (GMPKU-P-3753) shows three lateral

129

cusplets on the mesial side and eight lateral cusplets on the distal side (Figs. 3P-T). A mesiodistal crest

130

runs through the apices of the main cusp and lateral cusplets. One or two vertical ridges originate from

131

the longitudinal crest at each apex on both labial and lingual crown surfaces. These ridges fuse basally

132

with a horizontal circumferential rim developed along the entire crown shoulder. The crown/root

133 junction is marked with a groove labially and lingually.

134 The root is lower than the crown in anterolateral and lateral teeth, but its height is nearly equal to that
135 of the crown in posterior teeth (Fig. 3U). The root displays foramina of varying size that are arranged
136 in a row on the lingual root wall (Figs. 3F, K, U). Labially, foramina are irregularly distributed: they
137 are present at the basolabial edge in anterior and anterolateral teeth (Figs. 3B, L), whereas they are
138 restricted to the upper part of the root in posterior teeth (Fig. 3V). The basal root surface is flat and
139 displays a series of parallel canals at the labialmost part (Figs. 3N, X). The root vascularization is
140 anaulacorhize on the labial and lingual walls, but it resembles pseudopolyaulacorhize in basal view
141 with parallel canals that are open on the labialmost part. It differs from the latter vascularization system
142 by the absence of a corrugated basal root in labial view.

143 **Enameloid microstructure**—The enameloid consists of a single crystallite enameloid (SCE) made of
144 short rod-shaped units (Figs. 3Z-B'). The crystallites are varying in length between 0.3 and 0.5 μm .
145 Their arrangement does not change at the level of the vertical ridges (Fig. 3A') and longitudinal crest
146 (Fig. 3B'). The orthodentine was exposed once the enameloid was completely removed (Fig. 3C').

147 **Remarks**—The genus *Omanoselache* was erected by Koot et al. (2013) from the Wordian, Middle
148 Permian of Oman. The material described here matches well the monognathic heterodonty pattern of
149 *Omanoselache* in having symmetrical and basally arched anterior and anterolateral teeth, and
150 asymmetrical and straight lateral and posterior teeth. They are further assigned to *Omanoselache halli*
151 from the upper Olenekian of Oman by having a fusiform outline, pyramidal main cusp with a blunt
152 apex, circumferential rim, prominent lingual peg and small or absent labial peg, well developed
153 longitudinal crest and anaulacorhize to perhaps pseudopolyaulacorhize vascularization (Koot et al.,
154 2015). However, *Omanoselache halli* displays a stronger lingual peg and more separated cusplets.

155 Additionally, one lateral tooth (GMPKU-P-3752) displays three lateral cusplets on the mesial side and
156 eight on the distal side, which is more asymmetric than any teeth of *Omanoselache halli* recovered
157 from Oman. These differences are herein considered intraspecific variations. The tooth attributed to
158 *Polyacrodus tiandongensis* by Wang et al. (2001) from the same layers at Zuodeng locality shares the
159 above-mentioned crown characteristics with the material described here (a labial accessory process of
160 the crown described in the original paper is actually a lingual peg, because mesial and /or distal ends of
161 the crown are usually recurved linguallly, see figs. 5a-c; pl. 1, figs. Fa-Fc). However, one poorly
162 described crown lacking the root is difficult to diagnose. Besides, Fischer (2008) considered that
163 *Polyacrodus tiandongensis* might belong to *Lissodus angulatus*. However, numerous vertical ridges
164 and a prominent lingual peg in *Polyacrodus tiandongensis* separate it from *Lissodus angulatus*, which
165 displays less-developed vertical ridges of the crown and a moderate labial peg (Duffin, 1985). It is
166 here suggested that *Polyacrodus tiandongensis* is a *nomen dubium* and could possibly be attributed to
167 *Omanoselache halli*. Five teeth of *Lissodus* sp.1 previously described by Yamagishi (2006) were
168 already included into *Omanoselache halli* (Koot et al., 2015).

169 **Occurrence**—Upper Olenekian (Lower Triassic) of Oman (Yamagishi, 2006; Koot et al., 2015) and
170 Tiandong County, Guangxi Province, South China.

171

172 Genus HYBODUS Agassiz, 1837

173 *HYBODUS* sp. (Figure 4A-U)

174 **Material**—Four teeth, GMPKU-P-3780-83, from layers 8-11 of the Luolou Formation, Zuodeng
175 section. GMPKU-P-3783 was used for SEM microstructural study.

176 **Description**—The teeth measure 0.6-1.2 mm mesiodistally, 0.3-0.7 mm labiolingually and 0.9-1.3 mm

177 apico-basally. The crown consists of one main cusp flanked by one to three pairs of lateral cusplets.
178 The main cusp is upright (Figs. 4E, S) or slightly inclined lingually (Figs. 4J, O), about two to three
179 times as high as the lateral cusplets. The latter are situated slightly labially to the main cusp in
180 GMPKU-P-3780 (Fig. 4E), whereas all cusps are aligned in GMPKU-P-3782 except an outermost
181 cusplet that is slightly displaced labially (Fig. 4O) and overhangs the root (Fig. 4N). The main cusp is
182 slender with a sharply pointed apex (Figs. 4C, H). The adjacent cusplets are not completely separated
183 from each other. The crown surface is ornamented by rectilinear ridges that start from the apex and
184 reach the crown/root boundary. Each cusp bears two lateral cutting edges and two to three coarse ridges
185 on both labial and lingual surfaces (Figs. 4A-B, K-L). There is a groove that separates the crown from
186 the root labially (Fig. 4O) but it is absent lingually.

187 The root is largely damaged or missing in most specimens. However, GMPKU-P-3782 shows a low
188 root that protrudes lingually. A row of foramina is located on both labial and lingual root wall. Some
189 large and unroofed canals are exposed on the lingual root edge (Fig. 4K) and labio-basal part of the
190 root (Fig. 4N) due to the artificial damage.

191 **Enameloid microstructure**—The enameloid consists of a layer of single crystallite enameloid (SCE).
192 Each crystallite is 0.5-1 μm long, rod-shaped and randomly oriented at the cutting edge (Fig. 4T) and
193 on the labial face of the main cusp (Fig. 4U).

194 **Remarks**—The assignment of the material herein described to *Hybodus* is based on well-developed
195 slender cusplets, decreasing in height from the central main cusp to the lateral cusplets and a fairly
196 shallow root (Maisey, 1987; Duffin, 1993; Ginter et al., 2010). The aligned cusplets and coarse
197 rectilinear ridges are reminiscent of the ornamentation pattern of *Hybodus plicatilis* that was recorded
198 from the Middle-Late Triassic of Germany (Agassiz, 1843), Switzerland (Meyer, 1849; Rieppel, 1981),

199 Luxemburg (Delsate, 1992, 1993) and Spain (Pla et al., 2013; Manzanares et al., 2018, 2020). However,
200 GMPKU-P-37080-83 lack the deep root of *Hybodus plicatilis*, a diagnostic feature of the species.
201 Additionally, this species was transferred to the genus *Parhybodus* and considered as a neoselachian
202 because it displays a labially protruding root, and lacks a clear sulcus (groove) separating the crown
203 from the root on the labial face as in most species of *Hybodus* (Jaekel, 1898; Böttcher, 2015). Herein,
204 the root does not protrude labially, and is separated from the crown by a labial groove. It is therefore
205 better assigned to *Hybodus* than to *Parhybodus*. The overhanging outermost lateral cusplet separates it
206 from other *Hybodus* species, but such a characteristic is not sufficient to erect a new species. Thus, we
207 tentatively attribute these teeth to *Hybodus* sp. pending better material for a definite determination.

208 **Occurrence**—Upper Olenekian (Lower Triassic) of Tiandong County, Guangxi Province, South
209 China.

210

211 EUSELACHII incertae sedis

212 Genus *FAVUSODUS* Li and Cuny in Li et al., 2021

213 *FAVUSODUS ORIENTALIS* Li and Cuny in Li et al., 2021

214 (Figures 4V-W; 5A-P)

215 2004 *Acrodus* sp. e.g. *spitzbergensis* [sic] Yamagishi, pp. 565-574, figs. 3, 4a-b.

216 **Material**—Five teeth, GMPKU-P-3771-75, from layers 9-11 of the Luolou Formation, Zuodeng
217 section. GMPKU-P-3771-74 were used for imaging. GMPKU-P-3775 was used for SEM
218 microstructural study.

219 **Description**—The teeth are rather large and blunt, of varying completeness. Of them, GMPKU-P-3772
220 is nearly complete, measuring 2.5 mm mesiodistally, 0.9 mm labiolingually and 0.8 mm apico-basally.

221 The crown has one prominent main cusp and at least two lateral cusplets (GMPKU-P-3773) or no
222 lateral cusplet (GMPKU-P-3774). The main cusp is pyramid or dome-shaped with a blunt apex (Figs.
223 5C, H, O). A lingual peg is present on the main cusp, overhanging the root. Well-defined ridges
224 originate from the apex of the main cusp and extend to the crown shoulder. Some ridges bifurcate and
225 then converge into a network, forming a few small concave pits on the labial surface of the main cusp
226 (Fig. 5G), whereas some are parallel to each other on the labial and lingual crown surfaces,
227 perpendicular to the longitudinal crest (e.g. GMPKU-P-3774, Fig. 5O). The latter runs across the crown
228 mesio-distally (Figs. 5C, O). The crown and root are separated by a groove labially and lingually (Fig.
229 5L).

230 The root is lower labially than lingually. The labial side of the root displays a row of small foramina
231 just below the crown (Figs. 5B, G), whereas the lingual side displays a series of large, drop-shaped
232 foramina (Figs. 5A, F, J). In basal view, the root surface is divided into labial and lingual parts. The
233 labial one is much depressed and penetrated by parallel unroofed canals that sometimes reach the
234 basolabial edge (Figs. 5D, I). The vascularization is therefore pseudopolyaulacorhize.

235 **Enameloid microstructure**—The enameloid is about 30-40 μm thick in longitudinal section, made of
236 crystallites mostly oriented perpendicular to the surface (Fig. 4V). In surface view, the crystallites
237 appear to be somewhat randomly oriented (Fig. 4W). The crystallites are about 0.5 μm in length.

238 **Remarks**—The attribution of the material to *Favusodus orientalis* Li and Cuny in Li et al., 2021 is
239 based on the presence of the following characters: rather blunt crown with one prominent main cusp
240 and much reduced lateral cusplets, an overhanging lingual peg, ornamentation pattern and
241 pseudopolyaulacorhize vascularization. The ornamentation of the teeth herein described display less
242 honeycombed pits compared with *Favusodus orientalis* from the Nimaigu section of Guizhou Province

243 (Li et al., 2021) and Ehime Prefecture of Japan (Yamagishi, 2004). This difference could be caused by
244 a preservation artefact or abrasion when preying on hard-shelled items.

245 **Occurrence**—Upper Olenekian (Lower Triassic) of Tiandong County, Guangxi Province, South China;
246 upper Ladinian (Middle Triassic) of Xingyi City, Guizhou Province, South China (Li et al., 2021);
247 Upper Olenekian (Lower Triassic) to lower Anisian (Middle Triassic) of Ehime Prefecture, southwest
248 Japan (Yamagishi, 2004).

249

250 EUSELACHII gen. et sp. indet.

251 (Figure 5Q-D')

252 **Materials**—Five teeth, GMPKU-P-3777-79, GMPKU-P-3792-93, from layers 9-11 of the Luolou
253 Formation, Zuodeng section. GMPKU-P-3777-79 and GMPKU-P-3792 were used for imaging.

254 **Description**—All teeth are badly damaged, measuring 0.8-1.2 mm mesiodistally, 0.2-0.4 mm
255 labiolingually and 0.3-0.4 mm apico-basally. The crown consists of one main cusp flanked by up to
256 three or four cusplets on each side. The main cusp is slightly higher than the first pair of lateral cusplets.
257 Small intermediate cusplets are usually present between the main cusp and the nearest lateral cusplets
258 (Figs. 5A', C'). One additional accessory cusplet is situated on the mesial extremity of the crown (Fig.
259 5Q). Most cusps are acute, slightly inclined distally. The crown ornamentation cannot be characterized
260 due to the poor preservation of the teeth. There is no well-marked groove at the crown/root boundary.

261 The root protrudes both labially and lingually (Fig. 5S). It is slightly arched in the central part. A row
262 of small foramina is present on the lingual face of the root (Figs. 5Q, U). The foramina of the labial
263 surface of the root cannot be distinguished due to their poor preservation in all available teeth. The
264 basal root surface is rather flat and presents foramina roughly organized in a row exposed on the labial

265 part (Fig. 5T). The vascularization is anaulacorhize.

266 **Remarks**—The material is reminiscent of an undetermined taxon of euselachian sharks from the
267 Ladinian (Middle Triassic) of Xingyi, Guizhou Province (Li et al., 2021). We tentatively assign them to
268 the same taxon of *Euselachii* gen. et sp. indet. as described by Li and Cuny in Li et al., 2021 because of
269 their cladodont-like crown that displays intermediate cusplets and outermost accessory cusplet among
270 the well-developed cusplets, and euselachian-type root (anaulacorhize) with both labially and lingually
271 protruding root wall.

272 **Occurrence**—Upper Olenekian (Lower Triassic) of Tiandong County, Guangxi Province, South China;
273 upper Ladinian (Middle Triassic) of Xingyi City, Guizhou Province, South China (Li et al., 2021).

274

275 Subcohort NEOSELACHII Compagno, 1977

276 Order SYNECHODONTIFORMES Duffin and Ward, 1993

277 Family incertae sedis

278 Genus *SAFRODUS* Koot and Cuny in Koot et al., 2015

279 *SAFRODUS TOZERI* Koot and Cuny in Koot et al., 2015

280 (Figures 6A-I'; 7K-M)

281 2004 *Synechodus* sp. Yamagishi, pp. 572-573, fig. 5.1-3.

282 **Materials**— Nine teeth, GMPKU-P-3762-68, GMPKU-P-3800-01 from layer 9 of the Luolou

283 Formation, Zuodeng section. Two specimens were used for SEM microstructural study:

284 GMPKU-P-3762 and GMPKU-P-3768.

285 **Description**—The teeth are 0.9-2.2 mm long mesiodistally, 0.3-0.5 mm wide labiolingually and

286 0.6-0.9 mm in height. A gradient monognathic heterodont dentition is deduced because anterior teeth

287 are mesiodistally short with a relatively high main cusp and slightly arched root, whereas the lateral
288 and posterior teeth are mesiodistally elongated with a rather low main cusp and a straight root. The
289 polycuspid crown displays one robust main cusp flanked by slender and low lateral cusplets. There are
290 one to three cusplets on the distal side and one to four on the mesial side. All cusps bear a pointed apex
291 and become slanted distally from anterior to posterior teeth. In apical view, the main cusp and lateral
292 cusplets are compressed labio-lingually (Figs. 6C, H, R). A continuous longitudinal crest traverses the
293 apex of each cusp. At the base of the main cusp, the longitudinal crest may display small, irregular
294 bumps (Figs. 6L, P, E'). The crown is ornamented by three to eleven vertical ridges, both labially and
295 lingually. These ridges originate from the base of each cusp and converge to its apex. The crown/root
296 junction presents a shallow groove labially (Figs. 6Q, F').

297 The root is low and projects lingually. It has a pseudopolyaulacorhize vascularization with a row of
298 foramina on both labial and lingual root walls. These foramina are usually larger and more developed
299 on the lingual face of the root than on the labial one. The basal face of the root presents a mesiodistal
300 depression in the labial-most part penetrated by a row of foramina, some of them reaching the
301 labio-basal edge (Figs. 6D, C').

302 **Enameloid microstructure**—The microstructural analysis of GMPKU-P-3762 reveals a layer of
303 single crystallites enameloid (SCE), which is composed of numerous long and slender crystallites. The
304 crystallites are randomly arranged within a plane that is parallel to the crown surface, but these
305 crystallites are not parallel to each other (Figs. 7K-M).

306 **Remarks**—The following features support an attribution to *Safrodus tozeri*: a gradient monognathic
307 heterodont dentition with a high main cusp and not well-separated lateral cusplets, well-defined vertical
308 ridges and a continuous longitudinal crest. The posterior teeth of the current materials resemble those

309 of *Euselachii* gen et sp. indet. in crown pattern with distally inclined cusplets. However, the
310 indeterminate Euselachian teeth described herein display small intermediate cusplets next to the main
311 cusp, which is not the case in *Safrodus tozeri*. The enameloid of the material described here shows no
312 bundles and consists entirely of SCE, which differs from those of Oman that is made of a
313 double-layered enameloid displaying single short-rodded crystallites and subparallel to parallel
314 crystalline bundles (SCE and PBE) (Koot et al., 2015). Herein, the lack of bundles is possibly
315 explained by the small size of the teeth, which appears to be strongly recrystallized, resulting in a
316 blurry enameloid surface (see Figs. 7K-M), which makes difficult to observe the details of the
317 structure.

318 Three teeth (Yamagishi, 2004, figs. 5. 1-3) attributed to *Synechodus* sp. from the Spathian (upper
319 Olenekian) to lower Anisian of southwest Japan share with *Safrodus tozeri* all the above-mentioned
320 features apart from their vertical ridges on the main cusp and cusplets that often bifurcate near the
321 crown shoulder. These teeth are better ascribed to *Safrodus tozeri* than to *Synechodus* sp. because of an
322 extensive arched root in anterolateral teeth and the absence of a labial crown overhang (Koot et al.,
323 2015). However, the additional two posterolateral teeth attributed to *Synechodus* sp. should be
324 excluded from *Safrodus* due to their extremely asymmetric crown with almost no lateral cusplets
325 (Yamagishi, 2004, figs. 5. 4-5).

326 **Occurrence**—Upper Olenekian (Lower Triassic) of Oman (Koot et al., 2015) and Tiandong County,
327 Guangxi Province, South China; Upper Olenekian (Lower Triassic) to lower Anisian (Middle Triassic)
328 Ehime Prefecture, southwest Japan (Yamagishi, 2004).

329

330 Genus POLYFACIODUS Koot and Cuny in Koot et al., 2015

331

POLYFACIODUS PANDUS Koot and Cuny in Koot et al., 2015

332

(Figure 7A-E)

333

Material—One tooth, GMPKU-P-3770, from layer 8 of the Luolou Formation, Zuodeng section.

334

Description—The tooth is 0.8 mm mesiodistally, 0.4 mm labiolingually and 0.5 mm apico-basally.

335

The symmetric crown is labio-lingually compressed and displays one main cusp flanked by one pair of

336

intermediate cusplets and two pairs of lateral cusplets. The main cusp is twice as high as the first pair

337

of lateral cusplets. A pair of small intermediate cusplets are situated between the main cusp and lateral

338

cusplets (Fig. 7C). All cusps are triangular in shape but their apexes are not preserved. Cusp and

339

cusplets are fused together at their bases and separated by V-shaped notches. Labially, the

340

ornamentation is characterized by some poorly preserved vertical ridges and a longitudinal

341

circumferential rim along the crown shoulder (Fig. 7B). The latter is convex upwards in the central part

342

of the crown. A small lingual peg is present at the base of the main cusp, connected to a weak ridge that

343

extends apicobasally (Fig. 7A). A deeply incised groove lies between the crown/root boundary labially

344

(Fig. 7B) but is absent lingually (Fig. 7A).

345

The root is arched with a corrugated basolabial edge (Fig. 7B). The lingual foramina, larger than the

346

labial ones, are arranged in a row. In the basal face of the root, two unroofed canals extend to the

347

labio-basal edge. The root vascularization seems therefore to be pseudopolyaulacorhize.

348

Remarks—The following features, including labiolingually compressed crown, small lingual peg on

349

the main cusp, weak circumferential rim along the shoulder and lingually protruding root with a

350

pseudopolyaulacorhize vascularization, support the attribution of the tooth described here to

351

Polyfaciodus pandus (Koot et al., 2015). Symmetric crown and arched root suggest that

352

GMPKU-P-3770 may represent an anterior tooth. A pair of small intermediate cusplets between the

353 main cusp and the following lateral cusplets can also be observed in the anterior teeth of *Polyfaciodus*
354 *pandus* from Oman (see Koot et al. 2015, figs. 9B, F). The presence of intermediate cusplets has been
355 considered as a transitional feature between ‘cladodont’ and neoselachian teeth (Li et al. 2021).

356 **Occurrence**—Upper Olenekian (Lower Triassic) of Oman (Koot et al., 2015) and Tiandong County,
357 Guangxi Province, South China.

358

359 Genus SYNECHODUS Woodward, 1888

360 *SYNECHODUS* aff. *TRIANGULUS* Yamagishi, 2004

361 (Figure 7F-J)

362 **Material**—One tooth, GMPKU-P-3769, from layer 8 of the Luolou Formation, Zuodeng section.

363 **Description**—An asymmetric, elongated tooth measuring 2.6 mm mesiodistally, 0.6 mm labiolingually
364 and 0.9 mm apico-basally. The crown consists of one main cusp flanked by one lateral cusplet on the
365 distal side and at least three lateral cusplets on the mesial side. The main cusp is three times as high and
366 broad as the lateral cusplets. All cusps are somewhat pointed and bent distally, with an acute angle of
367 about 50°. The crown is slightly compressed labio-lingually in apical view, displaying an acute
368 longitudinal crest mesio-distally (Fig. 7H). Each cusp bears one faint and short vertical ridge on the
369 labial face. Lingually, the ridge looks somewhat inclined and reaches the base of the cusp. There is no
370 obvious groove between the crown and root.

371 The root is low. There are a series of foramina on the lingual side of the root, whereas foramina are
372 indiscernible on the labial side. The lingual foramina form crevice canals and approach to the lingual
373 root edge (Fig. 7F). The basal root surface is slightly arched in the central part. Some foramina and
374 unroofed canals are scattered on the basal face of the root.

375 **Remarks**—The material is quite reminiscent of the posterior tooth of *Synechodus triangulus*
376 (Yamagishi, 2004: fig. 4. 2a-b). They share an asymmetric crown with more lateral cusplets on the
377 distal side (at least three) than on the mesial side (a single one), a labio-lingually compressed crown as
378 well as distally-inclined cusp and cusplets. However, GMPKU-P-3769 has no foramina on the labial
379 face of the root and no concave labial depression on the basal face of the root. Its main cusp is much
380 elongated and lower than that of *Synechodus triangulus*. Therefore, pending more material, the current
381 tooth is tentatively attributed to *Synechodus* aff. *triangulus*.

382 **Occurrence**—Upper Olenekian (Lower Triassic), Tiandong County, Guangxi Province, South China.

383 5. Discussion

384 5.1 Biostratigraphical distribution

385 The shark teeth studied here were collected from layers 8, 9 and 11 (Figs. 1C, D, 2A) of the
386 Luolou Formation following Yang et al (1984), and their biostratigraphical distributions were
387 investigated at ZD I and ZD II sections, respectively, following Yan's (2013) conodont
388 biostratigraphical zones. The layers 8 and 9 range from the conodont *Discretella discrete* Zone, to
389 *Icriospathodus collinsoni* Zone and then *Triassospathodus homeri* Zone at the ZD I section, which
390 spans across the Smithian-Spathian boundary, whereas the Layer 11 of the ZD II section lies in the
391 early Spathian conodont zones that range from the *Icriospathodus collinsoni* Zone to *Triassospathodus*
392 *homeri* Zone and then *Triassospathodus brochus* Zone (Figs. 2B, C). A total of nine shark taxa were
393 recovered, four of which are restricted to the early Spathian, coming from layer 9 of the ZD I section
394 and the layer 11 of the ZD II section (Fig. 2), including *Euselachii* gen et sp. indet., *Favusodus*
395 *orientalis*, *Polyfaciodus pandus*, and *Safrodus tozeri*. The *Euselachii* gen et sp. indet and *Favusodus*
396 *orientalis* were described from the latest Ladinian (late Middle Triassic) of the Zhuganpo Member (Li

397 et al., 2021), and their stratigraphic distribution is expanded from the Ladinian down to the Spathian.

398 The five other taxa range from the Smithian to the Spathian in layers 8, 9 and 11, i.e. ‘*Hybodus*’

399 *zoudengensis*, ‘*Hybodus*’ *yohi*, *Hybodus* sp., *Omanoselache halli* and *Synechodus* aff. *triangulus* (Fig.

400 2).

401 5.2 Palaeobiodiversity indicated by univariate statistical descriptors

402 The α -diversity ecological proxy has been commonly used for evaluating the palaeobiodiversity in

403 time and space (Fraiser and Bottjer, 2007; Hautmann et al., 2011; Derycke et al., 2014). Comparisons

404 of univariate statistical descriptors, including Simpson's Index (D), Shannon Index (H) and Evenness

405 (E), are herein made among three Smithian and Spathian (Early Triassic) chondrichthyan faunas that

406 display a trans-Tethyan distribution: Zuodeng in South China, Oman, and southwest Japan (Table 1,

407 Table S1). Therein, D measures the probability that two randomly-selected teeth from a given shark

408 fauna will belong the same taxa; H measures the uncertainty in predicting correctly the taxon of the

409 next shark tooth collected; E measures how similar the abundances of different taxa are in a shark

410 fauna. Additionally, relative abundance of major groups based on numbers of teeth are used to

411 calculate their proportion in a given fauna (see Fig. 8, Table S2).

412 5.2.1 Shark fauna from Zuodeng

413 Within the Early Triassic shark fauna of Zuodeng, seven tooth species have been identified.

414 Additionally, three more taxa (‘*Hybodus*’ *zoudengensis*, ‘*Hybodus*’ *yohi* and ‘*Polyacrodus*’

415 *tiandongensis*) were originally described from the same layers by Wang et al. (2001). Among them,

416 ‘*Hybodus*’ *zoudengensis* and ‘*Hybodus*’ *yohi* present small intermediate cusplets and crowns

417 ornamented by weak ridges (Li et al., 2021), which probably question their attribution to hybodonts by

418 Wang et al. (2001). We tentatively attributed them to euselachians and their reassessment is in progress

419 by one of us (J.C. Li). '*Polyacrodus*' *tiandongensis* is poorly preserved and difficult to diagnose. We
420 suggest (see above) that it could be closer to the genus *Omanoselache* than to either *Polyacrodus* or
421 *Lissodus*. As a result, nine genera are identified from the Zuodeng section, including two hybodonts
422 (*Omanoselache halli* and *Hybodus* sp.), three neoselachians (*Synechodus* aff. *triangulus*, *Polyfaciodus*
423 *pandus* and *Safrodus tozeri*) and four euselachians with indeterminate affinities (*Euselachii* gen et sp.
424 indet, *Favusodus orientalis*, '*Hybodus*' *zoudengensis* and '*Hybodus*' *yohi*). The low value of Simpson's
425 Index ($D=0.177$) for this fauna indicates a high species diversity and low dominance of each shark
426 genera. The H value is high ($H=1.918$), indicating that individuals are evenly distributed among the
427 shark genera. The evenness ($E=0.873$) is also high, which indicates that the abundance of individuals
428 among the shark genera is similar. Thus, the univariate statistical descriptors indicate that the shark
429 palaeocommunity in Zuodeng is taxonomically diverse and evenly distributed.

430 5.2.2 Shark fauna from Oman

431 The Early Triassic shark fauna of Oman was recovered from allochthonous carbonate build-ups
432 which originated from the platform margin and isolated platforms in the Hawasina Basin (Glennie,
433 2005). The fauna consists of two hybodonts (*Omanoselache halli*, cf. *Omanoselache* sp.) and five
434 neoselachians (*Polyfaciodus pandus*, cf. *Polyfaciodus pandus*, *Safrodus tozeri*, cf. *Safrodus tozeri* and
435 cf. *Amelacanthus* sp.) (Koot et al., 2015). The univariate statistical descriptors indicate that the shark
436 fauna of Oman displays medium values of species diversity ($H=0.960$) and dominance ($D=0.547$), as
437 well as evenness ($E=0.493$) (Table 1). It is less diverse than that of Zuodeng ($D=0.177$); individuals are
438 not evenly distributed among the different shark genera ($H=0.960$, $E=0.493$), whereas they are evenly
439 recovered from those of Zuodeng ($H=1.918$, $E=0.873$). Moreover, the Early Triassic shark fauna of
440 Oman is neoselachian-dominated (88%, i.e., number of teeth of neoselachians/total number of all teeth

441 in the fauna, see Fig. 8, Table S2), which separates it from other coeval shark faunas elsewhere (Koot
442 et al., 2015).

443 5.2.3 Shark fauna from southwest Japan

444 The elasmobranch remains from the Taho limestone of Ehime Prefecture, southwest Japan were
445 originally reported by Goto et al. (1996), and later on identified extensively by Yamagishi (2004, 2006).
446 The shark-bearing layers range from Smithian (Early Triassic) to Anisian (Middle Triassic) in age
447 (Koike, 1994), and occur within an exotic block representing Triassic seamount sediments of the
448 Panthalassa but possibly close to the South China block (Ando et al., 2001). So far, three tooth genera
449 (*Polyacrodus* 'minimus', *Acrodus* sp. e. g. *spitzbergensis* [sic] and *Synechodus* sp.) were described
450 from the Smithian to the Spathian (Goto et al., 1996; Yamagishi, 2004, 2006), of which
451 poorly-diagnosed taxa were revised: *Acrodus* sp. e. g. *spitzbergensis* [sic] was transferred to *Favusodus*
452 *orientalis* by Li et al. (2021) and three anterior teeth of *Synechodus* sp. were identified as those of
453 *Safrodus tozeri*. *Polyacrodus* 'minimus' of southwest Japan was initially noted by Goto et al. (1996)
454 and subsequently attributed to *Lissodus minimus* by Fischer (2008). However, images and description
455 of original specimen are still missing, and the latter species has so far been restricted to the Upper
456 Triassic (Duffin, 2001). This taxon is therefore problematic and excluded from our quantitative
457 analysis. Therefore, three euselachians are recognised, including two neoselachians (*Safrodus tozeri*
458 and *Synechodus* sp.) and one hybodont (*Favusodus orientalis*). From the Smithian to the Spathian, the
459 Japan shark fauna was dominated by neoselachians (*Safrodus tozeri* and *Synechodus* sp.) and was
460 almost devoid of hybodonts (see Fig. 8, Table S2). The Simpson index ($D=0.934$) indicates that this
461 shark palaeocommunity is not as diverse as that of Zuodeng ($D=0.177$). The Shannon index ($H=0.167$)
462 and Evenness ($E=0.152$) are much lower than in Zuodeng ($H=1.918$, $E=0.873$, Table 1), indicating that

463 these two eastern Tethyan shark communities have completely different values in species distribution.

464 The shark fauna of Zuodeng is more diverse than those of southwest Japan.

465 *5.2.4 Palaeobiodiversity distribution*

466 Within the trans-Tethyan ocean, the Early Triassic (Smithian-Spathian) chondrichthyan fauna of
467 Zuodeng closely resembles that of Oman, but is more diverse and evenly distributed than the latter.

468 Compared with the neoselachian-dominated fauna of Oman, the low dominance of the Zuodeng' shark
469 community indicates it lacks any typical disaster or opportunist taxa that usually flourish after a mass

470 extinction (Harris et al., 1996; Looy et al., 2001). Along the east coast of the Palaeotethys, the

471 palaeobiodiversity in Zuodeng is more important when compared to the adjacent southwest Japan area.

472 A rather high species diversity with a rather low dominance shark fauna in Zuodeng reflects the

473 presence of a favourable ecological environment in the Nanpanjiang Basin. The generic and species

474 richness of Oman's Early Triassic chondrichthyan fauna indicate that hybodont sharks were abundant

475 in shallow water limestones that were deposited around storm wave base, whereas neoselachians were

476 more common in pelagic sediments in deep water (Koot et al., 2015). Accordingly, an archipelagic sea

477 mixing shallow water from a carbonate platform and deep water from the Nanpanjiang Basin

478 (Lehrmann et al., 2003, 2015; Enos et al., 2006) may account for various habitats available for these

479 euselachian sharks.

480 **5.3 Palaeoecology**

481 Tooth morphology has been used to infer the ecology of chondrichthyan taxa in multiple studies

482 (e.g., Kent, 1994; Ciampaglio et al., 2005; Pla et al., 2013; Scheyer et al., 2014; Cooper et al., 2023).

483 Herein, three feeding strategies, including grasping-crushing, grasping-swallowing and sharp-grasping,

484 are identified by different combination of ten crown characteristics (Table S3). The chondrichthyan

485 taxa with grasping-crushing tooth includes *Favusodus orientalis* and *Omanoselache halli*. This type of
486 dentition presents slightly high crowned anterior teeth and much lower posterior teeth, the latter with
487 rather flat crown and well-defined vertical ridges and/or honeycombed pits, implying durophagous
488 feeding habits (Pla et al., 2013; Koot et al., 2015; Li et al., 2021) probably based on ammonoids,
489 gastropods and bivalves (Fig. 2). These durophagous sharks, like extant Rajiformes and
490 Myliobatiformes, may had inhabited on the seabed in shallow coastal environments (Pla et al., 2013;
491 Cappetta, 2012). Three taxa with grasping-swallowing behaviours, including '*Hybodus*' *zuodengensis*,
492 '*Hybodus*' *yohi* and *Euselachii* gen. et sp. indet., display a cladodont-like crown with a combination of
493 the following characteristics: multicusped crown, slender and little-ornamented cusplets, large notch
494 between adjacent cusplets and small intermediate cusplets. Sharks with such teeth are prone to grasp
495 preys and then swallow them whole (Williams, 2001) rather than to tear chunks of meat out of them.
496 These sharks may feed on some small bony fishes and conodonts. The sharp-grasping typed tooth is
497 represented by three neoselachians (*Synechodus* aff. *triangulus*, *Polyfaciodus pandus* and *Safrodus*
498 *tozeri*) and one hybodont shark (*Hybodus* sp.). These sharks possess a polycusped crown with sharp
499 pointed apex or acute cutting edge, or well-defined ridges of both labial and lingual crown surfaces.
500 These characteristics add a cutting function to a primarily grasping function, which contributes to hold
501 on the prey more tightly or cut flesh of some soft-body animals into pieces. The conodont animals and
502 other chondrichthyans recovered from the studied section are potential prey items for these carnivores.
503 However, no teeth exceed 1.3 mm in crown height and 2.5 mm in crown width (Table S3), indicating
504 that the nine shark species described here share a similar small body size. The Early Triassic sharks of
505 Zuodeng display therefore diverse feeding habits, including grasping-crushing, grasping-swallowing
506 and sharp-grasping dentitions, which to some extent demonstrate they were part of a complex food

507 chain.

508 **5.4 Palaeobiogeography**

509 Palaeobiogeographically, the shark fauna of Zuodeng shares some common taxa with the
510 Smithian-Spathian of Oman, Spathian-Anisian of southwest Japan and Ladinian-Carnian Xingyi shark
511 faunas (Table S4). Three species (*Omanoselache halli*, *Polyfaciodus pandus* and *Safrodus tozeri*) of
512 Zuodeng have been found in the Early Triassic (Smithian-Spathian) of Oman (Koot et al., 2015). Of
513 them, *Safrodus tozeri* and *Favusodus orientalis* are present in the Early-Middle Triassic
514 (Spathian-Anisian) of southwest Japan (Yamagishi, 2004). *Favusodus orientalis* and *Euselachii* gen et
515 sp. indet., were previously reported from the Middle-Late Triassic (Ladinian-Carnian) of Xingyi, China
516 (Li et al., 2021). The other taxa, including '*Hybodus*' *zuodengensis*, '*Hybodus*' *yohi*, *Hybodus* sp. and
517 *Synechodus* aff. *triangulus* are endemic to Zuodeng.

518 These results suggest trans-regional taxa were prevailing during the Early Triassic
519 (Smithian-Spathian). A hybodont and neoselachian shark combination (*Omanoselache halli*,
520 *Polyfaciodus pandus* and *Safrodus tozeri*) was coevally shared both in Oman in the western Neotethys
521 and Zuodeng in the eastern Palaeotethys (Fig. 8). Their rather small tooth size (not exceeding 3 mm in
522 mesiodistal length) suggest that these chondrichthyan genera are small-bodied coastal sharks. A
523 long-distance trans-Tethyan migration between western Neotethys and eastern Palaeotethys would
524 therefore argue for continuous appropriate ecological habitats (Manzanares et al., 2020). The coastal
525 margin along the Cimmerian microcontinents, including Turkey, Iran, Afghanistan, Tibet and Malaysia
526 (Sengör, 1984), had a potential to form continuous epicontinental shallow-marine environments (Sweet,
527 1970; Metcalfe, 1990; Horacek et al., 2007; Wu et al., 2007), which possibly served as a migration
528 route for the trans-Tethyan dispersal of Early Triassic sharks as shown in Figure 8. However, with the

529 increasing expansion of the Neotethys and shrinkage of the Palaeotethys (Zhao et al., 2018, Zhao et al.,
530 2019), the Cimmerian microcontinents continuously moved northward, which to some extent prevented
531 such a trans-Tethyan migration route. Meanwhile, it is not unexpected that a short-distance shark
532 dispersion occurred between the Zuodeng and southwest Japan, because they were located on the
533 eastern coast of Palaeotethys and, therefore, palaeogeographically close during the Early Triassic.

534 **6. Conclusions**

535 The Zuodeng section in Guangxi area in South China has yielded abundant elasmobranch remains,
536 recording a diverse fauna with nine tooth taxa. Two hybodonts (*Omanoselache halli* and *Hybodus* sp.),
537 three neoselachians (*Safrodus tozeri*, *Polyfaciodus pandus* and *Synechodus* aff. *triangulus*) and four
538 euselachians of uncertain affinities (*Euselachii* gen. et sp. indet., *Favusodus orientalis*, '*Hybodus*' *yohi*
539 and '*Hybodus*' *zuodengensis*) are identified. *Polyacrodus tiandongensis* is here considered a *nomen*
540 *dubium*. The stratigraphical distribution of each taxon indicate an age comprised in the
541 Smithian-Spathian interval. The statistical analysis of shark palaeobiodiversity and palaeoecology
542 shows a high abundance and evenness, a low dominance in community constituent, as well as
543 diversified feeding strategies of grasping-crushing, grasping-swallowing and sharp-grasping. The
544 diversity of the fauna may be explained by an archipelagic ecological environment within the
545 Nanpanjiang Basin. Trans-regional taxa from Zuodeng and Oman suggest the Cimmerian
546 microcontinent may have behaved like a dispersal channel for shark migration between the eastern
547 Palaeo-Tethys and western Neo-Tethys during the Smithian and Spathian.

548 **Acknowledgements**

549 This study was financially supported by the National Natural Science Foundation of China (No.
550 42172009, 41920104001, 41876124), China Geological Survey (no. 121201102000150012-09), State

551 Key Laboratory of Palaeobiology and Stratigraphy, Nanjing Institute of Geology and Palaeontology,
552 CAS (No. 123107, 143108, 173123, 20182107) and China Scholarship Council (No. 202206010129).
553 We would like to thank Dr. Chai Jun (Peking University), Luo Denggao and Lu Jinyou (inhabitants of
554 Denggaolin village) for collecting rock samples in the field, and also Wang Mingcui for dissolving the
555 rock samples and picking up shark remains in the laboratory.

556 **Author contributions**

557 Jiachun Li: Conceptualization, Investigation, Formal analysis, Methodology and Writing- original draft.
558 Zuoyu Sun: Resources, Funding acquisition, Conceptualization and Writing- review & Editing. Gilles
559 Cuny: Writing- review & Editing and Conceptualization. Dayong Jiang: Supervision, Funding
560 acquisition.

561 **References**

- 562 Agassiz, L., 1833-1844. Recherches sur les Poissons Fossiles, 1-5. Imprimerie Petitpierre, Neuchâtel,
563 Switzerland, pp.1420.
- 564 Ando, A., Kodama, K., Kojima, S., 2001. Low-latitude and Southern Hemisphere origin of Anisian
565 (Triassic) bedded chert in the Inuyama area, Mino terrane, central Japan. Journal of Geophysical
566 Research 102, 1973-1986.
- 567 Bengtson, P., 1988. Open nomenclature. Palaeontology 31, 223-227.
- 568 Birkenmajer, K., Jerzmańska, A., 1979. Lower Triassic shark and other fish teeth from Hornsund,
569 south Spitsbergen. Studia Geologica Polonica 40, 7-37.
- 570 Błazejowski, B., 2004. Shark teeth from the Lower Triassic of Spitsbergen and their histology. Polish
571 Polar Research 25, 153-167.
- 572 Bonaparte, C.L.J., 1838. Selachorum tabula analytica. Nuovi Annali delle Scienze Naturali Bologna 1,

573 195-214.

574 Bratvold, J., Lene Liebe D., Hurum, J. H., 2018. Chondrichthyans from the *Grippia* bonebed (Early
575 Triassic) of Marmierfjellet, Spitsbergen. *Norwegian Journal of Geology* 98,189-217.

576 Böttcher, R., 2015. Fische des Lettenkeuper. *Der Lettenkeuper—Ein Fenster in die Zeit vor den*
577 *Dinosauriern. Palaeodiversity, Sonderband 2015*, 141-202.

578 Cappetta, H., 2012. Chondrichthyes (Mesozoic and Cenozoic Elasmobranchii: teeth). *Handbook of*
579 *paleoichthyology, Vol. 3E. Friedrich Pfeil*, pp. 512.

580 Chen, Z.Q., Benton, M.J., 2012. The timing and pattern of biotic recovery following the end-Permian
581 mass extinction. *Nature Geoscience* 5, 375-383.

582 Ciampaglio, C., Wray, G., Corliss, B., 2005. A toothy tale of evolution: Convergence in tooth
583 morphology among marine Mesozoic–Cenozoic sharks, reptiles, and mammals. *The Sedimentary*
584 *Record* 3, 4-8.

585 Compagno, L.J.V., 1977. Phyletic relationships of living sharks and rays. *American Zoologist* 17,
586 303-322.

587 Cooper, J.A., Griffin, J.N., Kindlimann, R., Pimiento, C., 2023. Are shark teeth proxies for functional
588 traits? A framework to infer ecology from the fossil record. *Journal of Fish Biology*. [https://doi.](https://doi.org/10.1111/jfb.15326)
589 [10.1111/jfb.15326](https://doi.org/10.1111/jfb.15326).

590 Cuny, G., Rieppel, O., Sander, P. M., 2001. The shark fauna from the Middle Triassic (Anisian) of
591 North-Western Nevada. *Zoological Journal of the Linnean Society* 133, 285-301.

592 Delsate, D., 1992. Chondrichthyens Mésozoïques du Luxembourg. Note préliminaire. *Bulletin de la*
593 *Société des Naturalistes Luxembourgeois* 93, 181-193.

594 Delsate, D., 1993. Synthèse des faunes d'Elasmobranches du Trias et du Jurassique de Lorraine.

595 Cossmanniana, Hors-série 2, 52-55.

596 Derycke, C., Olive, S., Groessens, E., Goujet, D., 2014. Paleogeographical and paleoecological
597 constraints on Paleozoic vertebrates (chondrichthyans and placoderms) in the ardenne massif;
598 shark radiations in the Famennian on both sides of the palaeotethys. *Palaeogeography,*
599 *Palaeoclimatology, Palaeoecology* 414, 61-67.

600 Duffin, C.J., 1985. Revision of the hybodont selachian genus *Lissodus* Brough (1935).
601 *Palaeontographica. Abteilung A* 188, 105-152.

602 Duffin, C.J., 1993. Mesozoic Chondrichthyan faunas 1. Middle Norian (Upper Triassic) of Luxemburg.
603 *Palaeontographica. Abteilung A* 229,15-36.

604 Duffin, C.J., Ward, D.J., 1993. The Early Jurassic paleospinacid sharks of Lyme Regis, southern
605 England. *Belgian Geological Survey, Professional Paper* 264, 53-102.

606 Duffin, C.J., 2001. Synopsis of the selachian genus *Lissodus* Brough, 1935. *Neues Jahrbuch für*
607 *Geologie und Paläontologie, Abhandlungen, Stuttgart* 221, 145-218.

608 Enault, S., Guinot, G., Koot, M.B., Cuny, G., 2015. Chondrichthyan tooth enameloid: past, present, and
609 future. *Zoological Journal of the Linnean Society* 174, 549-570.

610 Enos, P., Lehrmann, D.J., Wei, J. Y., Yu, Y.Y., Xiao, J.F., Chaikin, D. H., Minzoni, M., Berry, A.K.,
611 Montgomery, P., 2006. Triassic Evolution of the Yangtze Platform in Guizhou Province, People's
612 Republic of China. *Geological Society of America, Special Papers* 417,1-105.

613 Erwin, D. H., 1993. The great Paleozoic crisis: life and death in the Permian. Columbia University
614 Press.

615 Fan, J.X., Shen, S.Z., Erwin, D.H., Sadler, P.M., MacLeod, N., Cheng, Q.M., Hou, X.D., Yang, J.,
616 Wang, X.D., Wang, Y., Zhang, H., Chen, X., Li, G.X., Zhang, Y.C., Shi, Y.K., Yuan, D.X., Chen,

617 Q., Zhang, L.N., Li, C., Zhao, Y.Y., 2020. A high-resolution summary of Cambrian to Early
618 Triassic marine invertebrate biodiversity. *Science* 367, 272-277.

619 Fraiser, M. L., Bottjer, D. J., 2007. Elevated atmospheric CO₂ and the delayed biotic recovery from the
620 end-Permian mass extinction. *Palaeogeography, Palaeoclimatology, Palaeoecology* 252(1-2),
621 164-175.

622 Fischer, J., 2008. Brief synopsis of the hybodont form taxon *Lissodus* Brough, 1935, with remarks on
623 the environment and associated fauna. *Freiberger Forschungshefte C* 528,1-23.

624 Ginter, M., Hampe, O., Duffin, C.J., 2010. Chondrichthyes—Paleozoic Elasmobranchii: teeth; in H-P.
625 Schultze (ed.), *Handbook of Paleoichthyology 3D*. Verlag Dr. Friedrich Pfeil, Munich, pp. 168.

626 Glennie, K.W., 2005. *The Geology of the Oman Mountains—an outline of their origin*. Second edition.
627 Scientific Press Ltd, Beaconsfield, pp. 110.

628 Goto, M., 1994. Palaeozoic and early Mesozoic fish faunas of the Japanese Islands. *The Island Arc* 3(4),
629 247-254.

630 Goto, M., Uyeno, T., Yabumoto, Y., 1996. Summary of Mesozoic elasmobranch remains from Japan;
631 pp. 73-78 in G. Arratia and A. Tintori (eds.), *Mesozoic Fishes-Systematic and Paleoecology*.
632 Verlag Dr. Friedrich Pfeil, München.

633 Goto, M., Tanaka, T., Utsunomiya, S., 2010. On a tooth remain of *Lissodus* (Elasmobranchii) from the
634 Taho Formation (Lower Triassic) in Seiyo City, Ehime Prefecture, southwest Japan. *Earth Science*
635 64, 111-116. [in Japanese with English abstract]

636 Guinot, G., Adnet, S., Cavin, I., Cappetta, H., 2013. Cretaceous stem chondrichthyans survived the
637 end-Permian mass extinction. *Nature Communications* 4, 1-8.

638 Harris, P.J., Kauffman, E.G., Hansen, T.A., 1996. Models for biotic survival following mass

639 extinctions; pp. 41-60 in M.B. Hart (ed.), Biotic recovery from mass extinction events. Geological
640 Society. Special Publication 102, London.

641 Hautmann, M., Bucher, H., Bruchwiler, T., Goudemand, N., Kaim, A., Nuetzel, A., 2011. An unusually
642 diverse mollusc fauna from the earliest Triassic of South China and its implications for benthic
643 recovery after the end-Permian biotic crisis. *Geobios* 44(1), 71-85.

644 Hay, O.P., 1902. Bibliography and catalogue of the fossil vertebrata of North America. United States
645 Geological Survey, Bulletin 179, 18-68.

646 Horacek, M., Richoz, S., Brandner, R., Krystyn, L., Spötl, C., 2007. Evidence for Recurrent Changes in
647 Lower Triassic Oceanic Circulation of the Tethys: The $\delta^{13}\text{C}$ Record from Marine Sections in Iran.
648 *Palaeogeography, Palaeoclimatology, Palaeoecology* 252(1/2), 355-369.
649 <https://doi.org/10.1016/j.palaeo.2006.11.052>.

650 Huxley, T.H., 1880. On the application of the laws of evolution to the arrangement of the Vertebrata,
651 and more particularly of the Mammalia. *Proceedings of the Zoological Society of London* 1880,
652 649-662.

653 Jaekel, O., 1898. Ueber *Hybodus*. – *Sitzungs-Berichte der Gesellschaft naturforschender Freunde zu*
654 *Berlin*, 1898, 135-146.

655 Kasumzadeh, A.A., 2000. Sostojanié izuchennosti triasovykh otlozhenij Azerbaidzhana i problemy
656 granizy permi i triasa [Advances in research of the Triassic deposits in Azerbaijan and problems
657 of the Permian-Triassic boundary]. Baku: Nafta-Press. pp. 116.

658 Kato, T., Hasegawa, K., Ishibashi, T., 1995. Discovery of Early Triassic hybodontoid shark tooth from
659 the southern Kitakami Massif. *Journal of Geological Society of Japan* 101(6), 466-469. [in
660 Japanese]

661 Kent, B. W., 1994. Fossil sharks of the Chesapeake Bay region. Columbia, Maryland: Egan Rees &
662 Boyer, Inc.145.

663 Koike, T., 1994. Skeletal apparatus and its evolutionary trends in a Triassic conodont *Ellisonia*
664 *dinodooides* (Tatge) from the Tahoe Limestone, Southwest Japan. Transactions and Proceedings of
665 the Palaeontological Society of Japan, New Series 173, 366-383.

666 Koot, M.B., 2013. Effects of the Late Permian mass extinction on chondrichthyan palaeobiodiversity
667 and distribution patterns. Unpublished PhD thesis, Plymouth University, pp. 853.

668 Koot, M.B., Cuny, G., Tintori, A., Twitchett, R.J., 2013. A new diverse shark fauna from the Wordian
669 (Middle Permian) Khuff Formation in the interior Haushi–Huqf area, Sultanate of Oman.
670 Paleontology 56, 303-343.

671 Koot, M.B., Cuny, G., Tintori, A., Twitchett, R.J., 2015. New hybodontiform and neoselachian sharks
672 from the Lower Triassic of Oman. Journal of Systematic Paleontology 13, 891-917.

673 Lehrmann, D.J., Payne, J.L., Felix, S., Dillett, P.M., Wang, H., Yu, Y., Wei, J., 2003. Permian -Triassic
674 boundary sections from shallow-marine carbonate platforms of the Nanpanjiang Basin, South
675 China: implications for oceanic conditions associated with the end-Permian extinction and its
676 aftermath. Palaeogeography. Palaeoclimatology. Palaeoecology 18, 138-152.

677 Lehrmann, D.J., Bentz, J.M., Wood, T., Goers, A., Dhillon, R., Akin, S., Li, X.W., Payne, J.L., Kelley,
678 B.M., Meyer, K.M., Schaal, E.K., Suarez, M.B., Yu, M.Y., Qin, Y.J., Li, R.X., Minzoni, M.,
679 Henderson, C.M., 2015. Environmental controls on the genesis of marine microbialites and
680 dissolution surface associated with the end-Permian mass extinction: new sections and observations
681 from the Nanpanjiang Basin, South China. Palaios 30, 529-552.

682 Li, J.C., Sun, Z.Y., Cuny, G., Ji, C., Jiang, D.Y., Zhou, M., 2021. An unusual shark assemblage from

683 the Ladinian-Carnian interval of South China. Papers in Palaeontology.
684 <https://doi.org/10.1002/spp2.1404>.

685 Looy, C.V., Twitchett, R.J., Bilcher, D.L., van Konijnenburg-van Cittert, J.H.A., Visser, H., 2001. Life
686 in the end-Permian dead zone. Proceedings of the National Academy of Science 98, 7879-7883.

687 Lyu, Z., Orchard, M.J., Golding, M.L., Henderson, C.M., Chen, Z.Q., Zhang, L., Han, C., Wu, S.L.,
688 Huang, Y.G., Zhao, L.S., Bhat, G.M., Baud, A., 2021. Lower Triassic conodont biostratigraphy of
689 the Guryul Ravine section, Kashmir. Global and Planetary Change 207, 103671.

690 Maisey, J.G., 1987. Cranial anatomy of the Lower Jurassic shark *Hybodus reticulatus* (Chondrichthyes:
691 Elasmobranchii), with comments on hybodontid systematics. American Museum Novitates 2878,
692 1-39.

693 Manzanares, E., Pla, C., Ferrón, H., Botella, H., 2018. Middle-Late Triassic chondrichthyan remains
694 from the Betic Range (Spain). Journal of Iberian Geology 44 (1), 129-138.

695 Manzanares, E., Escudero-Mozo, M.J., Ferrón, H., Martínez-Pérez, C., Botella, H., 2020. Middle
696 Triassic sharks from the Catalan Coastal ranges (NE Spain) and faunal colonization patterns
697 during the westward transgression of Tethys. Palaeogeography, Palaeoclimatology, Palaeoecology
698 539. <https://doi.org/10.1016/j.palaeo.2019.109489>.

699 Metcalfe, I., 1990. Triassic Conodont Biostratigraphy in the Malay Peninsula. Geological Society of
700 Malaysia Bulletin 26, 133-45.

701 Meyer, H., 1849. Fossile Fische aus dem Muschelkalk von Jena, Querfurt und Esperst adt.
702 Palaeontographica 1, 195-208.

703 Mutter, R.J., Neuman, A.G., 2006. An enigmatic chondrichthyan with Paleozoic affinities from the
704 Lower Triassic of western Canada. Acta Palaeontologica Polonica 51(2), 271-282.

705 Mutter, R.J., Neuman, A.G., 2008. New eugeneodontid sharks from the Lower Triassic Sulphur
706 Mountain Formation of Western Canada; pp. 9-41 in L. Cavin, A. Longbottom and
707 M. Richter (eds.), Fishes and the Break-up of Pangaea. Geological Society, London, Special
708 Publications, 295.

709 Mutter, R.J., Neuman, A.G., 2009. Recovery from the end-Permian extinction event: evidence from
710 “Lilliput *Listracanthus*”. *Palaeogeography, Palaeoclimatology, Palaeoecology* 284, 22-28.

711 Mutter, R.J., Rieber, H., 2005. *Pyknotylacanthus spathianus* gen. et sp. nov., a new ctenacanthoid from
712 the Early Triassic of Bear Lake (Idaho, USA). *Revista Brasileira de Paleontologia* 8(2), 139-148.

713 Mutter, R.J., De Blanger, K., Neuman, A.G., 2007. Elasmobranchs from the Lower Triassic Sulphur
714 Mountain Formation near Wapiti Lake (BC, Canada). *Zoological Journal of the Linnean Society*
715 149, 309-337.

716 Mutter, R.J., Neuman, A.G., De Blanger, K., 2008. *Homalodontus* nom. nov., a replacement name for
717 *Wapitiodus* Mutter, de Blanger and Neuman, 2007 (Homalodontidae nom nov., ?Hybodontoida),
718 preoccupied by *Wapitiodus* Orchard, 2005. *Zoological Journal of the Linnean Society* 154,
719 419-420.

720 Nielsen, E., 1952. On new or little known Edestidae from the Permian and Triassic of East Greenland.
721 *Medd Gronl* 144, 1-55.

722 Obruchev, D.B., 1965. Razvitié i smena morskich organizmov na rubezhe paleozoja i mesozoja
723 [Development and change of marine organisms at the Palaeozoic-Mesozoic boundary] [in
724 Russian]. *Trudy Paleontologicheskii Institut* 108, 266-267.

725 Patterson, C., 1966. British Wealden sharks. *Bulletin of the British Museum (Natural History) Geology*
726 11, 283-349.

727 Pielou, E., 1966. The measurement of diversity in different types of biological collections. The Journal
728 of Theoretical Biology 13, 131-144.

729 Pitrat, C.W., 1973. Vertebrates and the Permo-Triassic extinction. Palaeogeography, Palaeoclimatology,
730 Palaeoecology 14, 249-264.

731 Pla, C., Márquez-Aliaga, A., Botella, H., 2013. The chondrichthyan fauna from the Middle Triassic
732 (Ladinian) of the Iberian Range (Spain). Journal of Vertebrate Palaeontology 33(4), 770-785.

733 Rieppel, O., 1981. The hybodont sharks from the Middle Triassic of Monte San Giorgio, Switzerland.
734 Neues Jahrbuch für Geologie und Palaontologie, Abhandlungen 161, 324-353.

735 Romano, C., Brinkmann W., 2010. A new specimen of the hybodont shark *Palaeobates polaris* with
736 three-dimensionally preserved Meckel's cartilage from the Smithian (Early Triassic) of
737 Spitsbergen. Journal of Vertebrate Paleontology 30, 1673-1683.

738 Romano, C., Koot, M.B., Kogan, I., Brayard, A., Minikh, A.V., Brinkmann, W., Bucher, H., Kriwet, J.,
739 2016. Permian-Triassic osteichthyes (bony fishes): diversity dynamics and body size evolution.
740 Biological Reviews 91, 106-147.

741 Scheyer, T.M., Romano, C., Jenks, J., Bucher, H., 2014. Early Triassic marine biotic recovery, the
742 predators' perspective. PLoS One 9(3), e88987.

743 Scotese, C.R., 2014. Paleomap Project: Early Triassic Paleomap. <http://www.scotese.com/newpage8.htm>.

744

745 Sengör, A.M.C., 1984. The Cimmeride Orogenic System and the tecton-ics of Eurasia. Geological
746 Society of America, Special Paper 195, 1-82.

747 Sepkoski, J.J., 1981. A factor analytic description of the Phanerozoic marine fossil record.
748 Paleobiology 7, 36-53.

- 749 Shannon, C.E., 1948. A mathematical theory of communication. Bell System Technical Journal 27,
750 466-467.
- 751 Simpson, E.H., 1949. Measurement of diversity. Nature 189, 688.
- 752 Stanley, S.M., 2016. Estimates of the magnitudes of major marine mass extinctions in earth history.
753 Proceedings of the National Academy of Sciences of the United States of America 113,
754 6325-6334.
- 755 Stensiö, E.A., 1918. Notes on some fish remains collected at Hornsund by the Norwegian Spitz-
756 bergen Expedition in 1917. Norsk Geologisk Tidsskrift 5, 75-78.
- 757 Stensiö, E.A., 1921. Triassic fishes from Spitsbergen. Part I. A. Holzhausen, Vienna, pp. 307.
- 758 Sweet, W.C., 1970. Uppermost Permian and Lower Triassic Conodonts of the Salt Range and
759 Trans-Indus Ranges, West Pakistan; pp 2017-275 in B. Kummel and C. Teichert (eds.),
760 Stratigraphic Boundary Problems: Permian and Triassic of West Pakistan. University of Kansas,
761 Department of Geology Special Publications, Kansas, America.
- 762 Thies, D., 1982. A neoselachian shark tooth from the Lower Triassic of the Kocaeli (= Bithynian)
763 Peninsula, West Turkey. Neues Jahrbuch für Geologie und Paläontologie, Monatshefte 1982,
764 272-278.
- 765 Thomson, K. S., 1982. An Early Triassic hybodont shark from Northern Madagascar. Postilla 186,
766 1-16.
- 767 Wang, N.Z., Yang, S.R., Jin, F., Wang, W., 2001. Early Triassic Hybodontoida from Tiandong of
768 Guangxi, China-first report on the fish sequence near the Permian-Triassic Boundary in South
769 China. Vertebrata Palasiatica 39, 237-250. [in Chinese with English abstract]

770 Williams, M.E., 2001. Tooth retention in cladodont sharks: with a comparison between primitive
771 grasping and swallowing, and modern cutting and gouging feeding mechanisms. *Journal of*
772 *Vertebrate Paleontology* 21, 214-226.

773 Woodward, A.S., 1888. On the Cretaceous selachian genus *Synechodus*. *Geological Magazine* 3,
774 496-499.

775 Wu, G. C., Yao, J. X., Ji, Z. S., 2007. Triassic Conodont Biostratigraphy in the Coqen Area, Western
776 Gangdise, Tibet, China. *Geological Bulletin of China* 26(8), 938-946 [in Chinese with English
777 Abstract].

778 Yamagishi, H., 2004. Elasmobranch remains from the Taho Limestone (Lower-Middle Triassic) of
779 Ehime Prefecture, Southwest Japan; pp. 565-574 in G. Arratia and A. Tintori (eds.), *Mesozoic*
780 *Fishes 3-Systematics, Paleoenvironments and Biodiversity*. Verlag Dr. Friedrich Pfeil, München.

781 Yamagishi, H., 2006. Permo-Triassic elasmobranch fauna: diversity, paleobiogeography and recovery
782 after the mass extinction. Unpublished PhD thesis, University of Tokyo, pp. 128.

783 Yamagishi, H., 2009. Chondrichthyans. pp.196-202 in Y. Shigeta, Y. D. Zakharov, H. Maeda and A. M.
784 Popov (eds.), *The Lower Triassic system in the Abrek Bay area, South Primorye, Russia*. National
785 Museum of Nature and Science Monographs, Tokyo, 38.

786 Yan, C., 2013. Study on Early-Middle Triassic conodont biostratigraphy in Nanpanjiang area:
787 [Dissertation]. China University of Geosciences, Wuhan, pp. 1-99. [in Chinese with English
788 abstract]

789 Yang, S.R., Wang, X.P., Hao, W.C., 1984. New knowledge of the Lower Triassic of Zuodeng,
790 Tiandong County of Guangxi Province, China; pp. 105-117 in T.K. Huang (ed.), *Selected Papers*
791 *in Honor of Prof. Yoh S.S. on the Sixty Years for his Geological Study and Education*. Beijing:

792 Geological Publishing House. [in Chinese]

793 Zhang, M.M., 1976. A new species of helicoprionid shark from Xizang. *Scientia Geologica Sinica*

794 1976, 332-336. [in Chinese with English abstract]

795 Zhao, G.C., Wang, Y.J., Huang, B.C., Dong, Y.P., Li, S.Z., Zhang, G.W., Yu, S., 2018. Geological

796 reconstructions of the East Asian blocks; from the breakup of Rodinia to the assembly of

797 Pangea. *Earth-Science Reviews* 186, 262-286.

798 Zhao, J., Huang, B.C., Yan, Y.G., 2019. The Middle–Late Triassic closure of the East Paleotethys

799 Ocean: Paleomagnetic evidence from the Baoshan Terrane, China. *Acta Geologica Sinica (English*

800 Edition) 93(6), 1978-1979.

801 Zhao, J.K., 1959. Ammonites from the Lower Triassic of western Guangxi. New species of

802 *Palaeontologia Sinica*, Volume 9, The Science Press, Beijing, China.

804 Table 1

805 Dominance and evenness of shark teeth.

	Zuodeng	Oman	Southwest Japan
Simpson index (D) ^a	0.177	0.547	0.934
Shannon Index (H) ^b	1.918	0.960	0.167
Evenness (E) ^c	0.873	0.493	0.152

806 ^a D values range from a minimum value of [1/total number of teeth in a fauna] to a maximum

807 value of 1; the larger the value of D, the lower the diversity and the higher the dominance of only

808 a few taxa.

809 ^b H values range from a minimum value of 0 to a maximum value of ln [total number of taxa in a

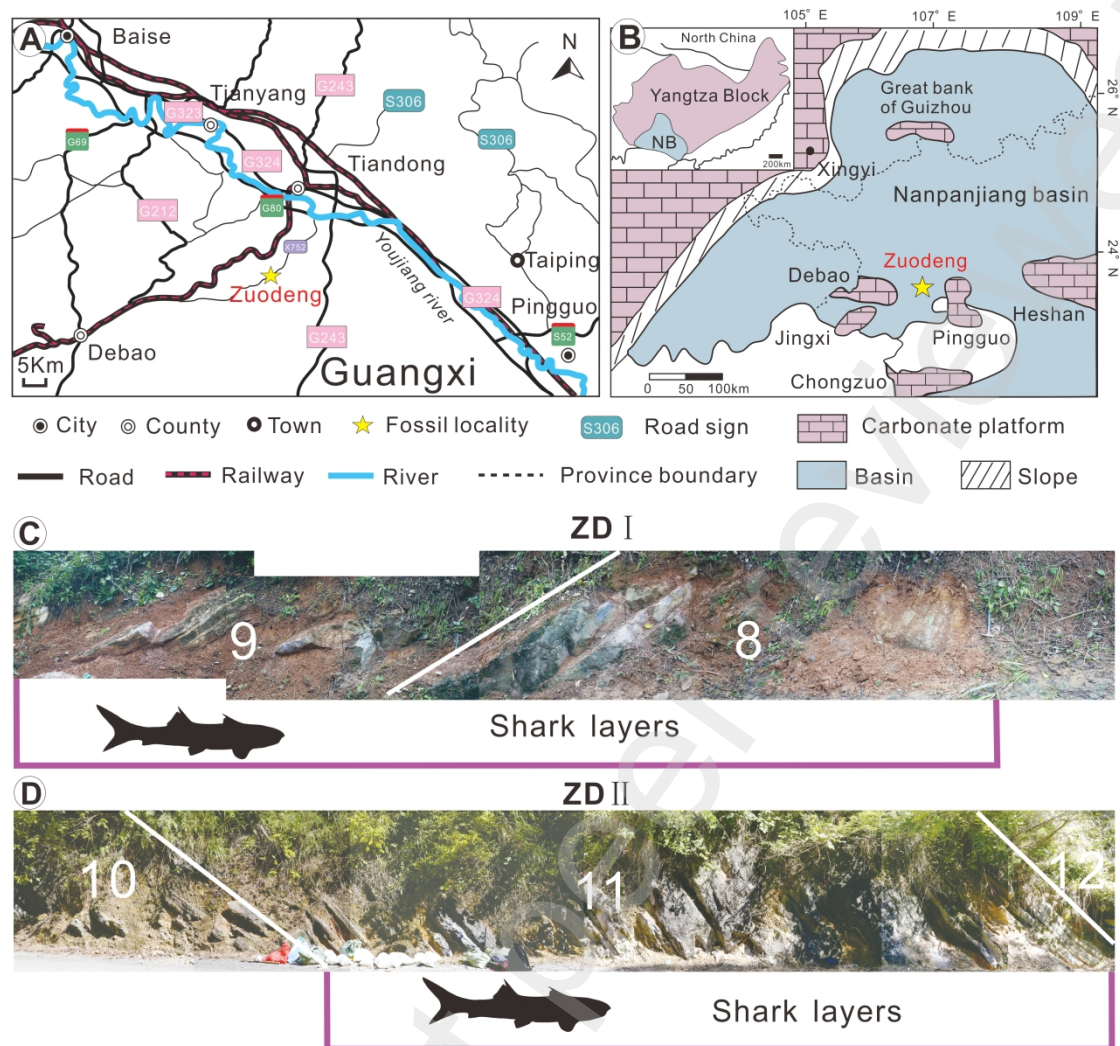
810 fauna] whereby higher values indicate that teeth are distributed more evenly among the taxa.

811 ^c E values range from a minimum value of 0 to a maximum value of 1 whereby higher values

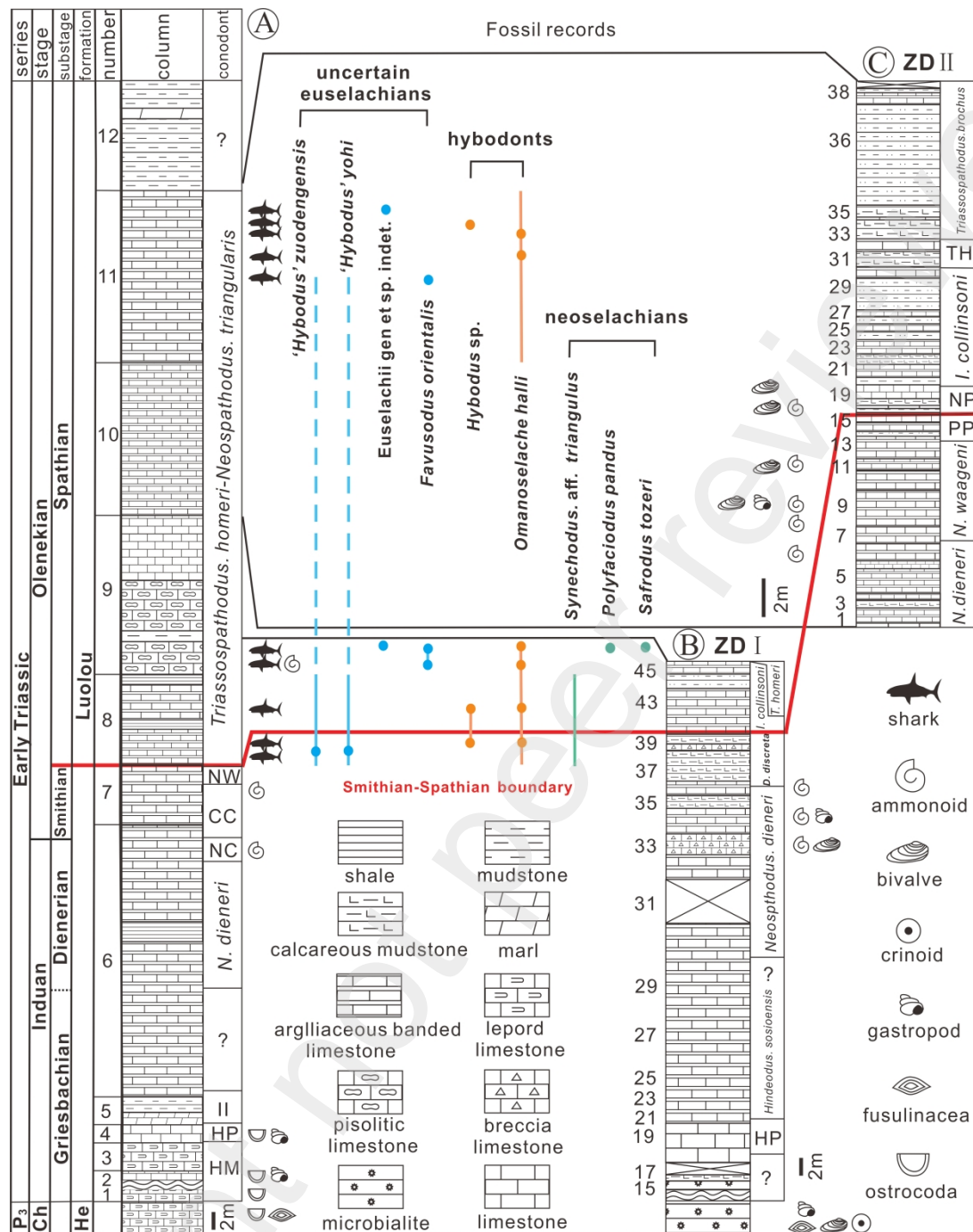
812 indicate similar proportions of teeth in the taxa, and lower values indicate dissimilar abundances

813 of teeth among the taxa.

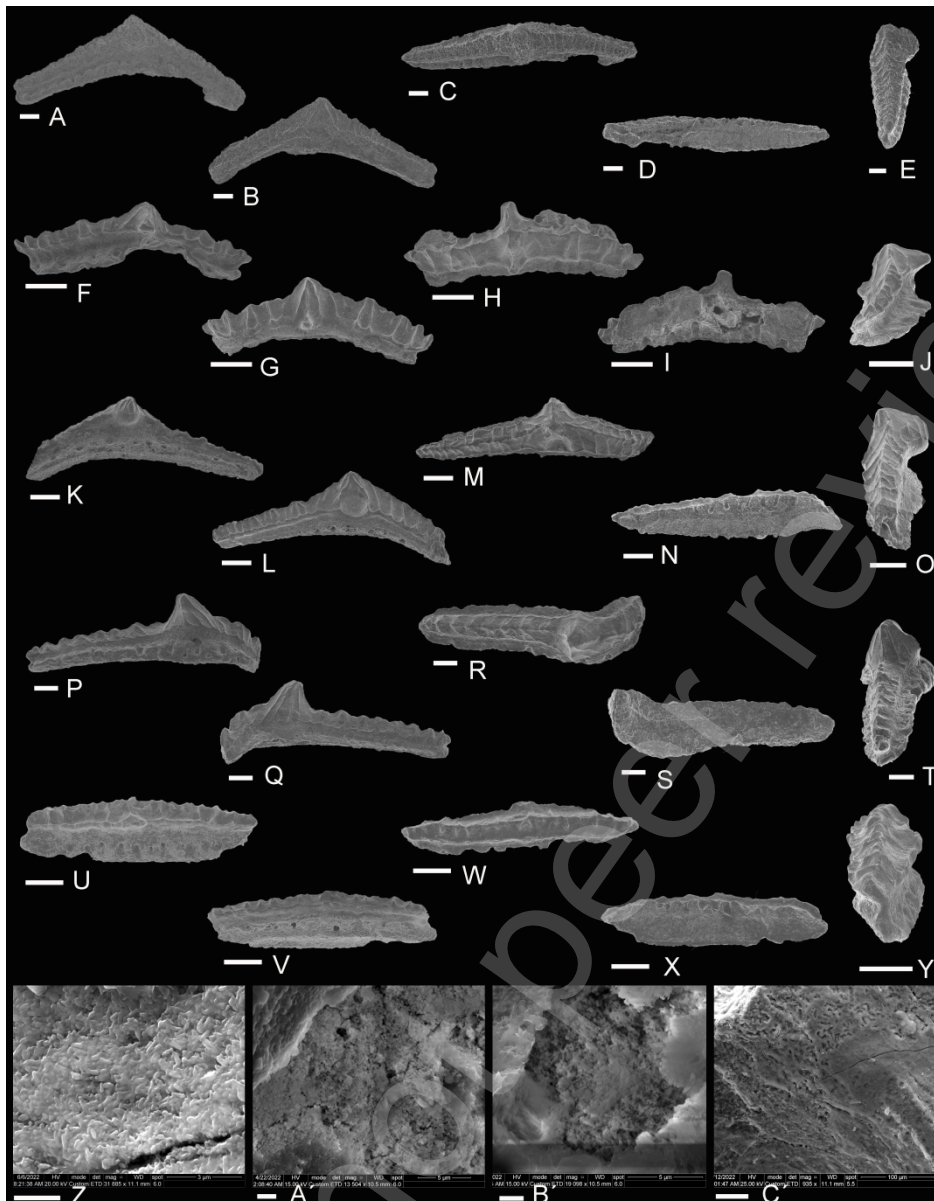
Preprint not peer reviewed



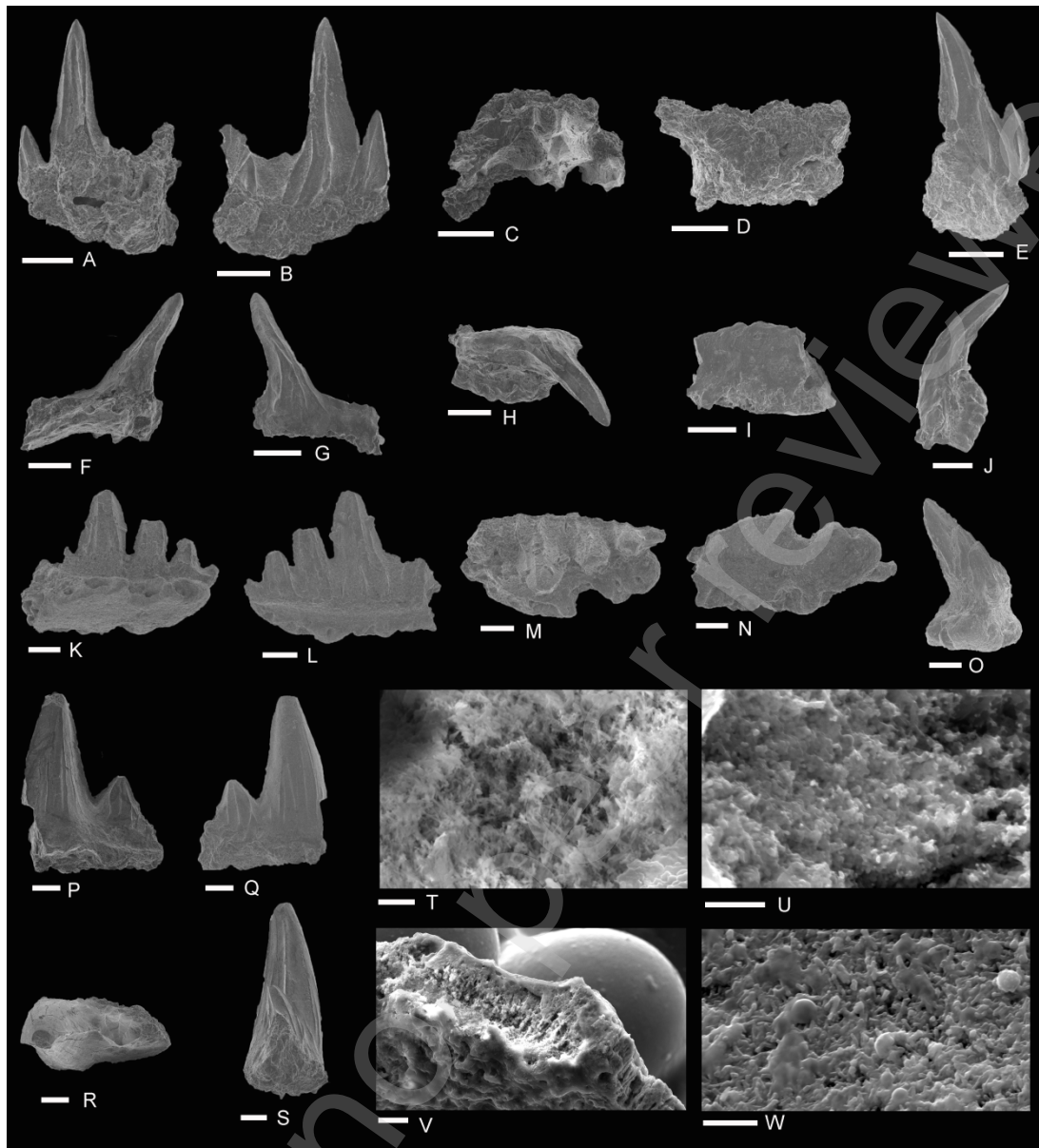
816 FIGURE 1. Geological setting and photograph of the Zuodeng section. **A**, showing the location of
 817 the Zuodeng locality, Tiandong County, Baise City, Guangxi Province. **B**, palaeogeographical
 818 map of the Nanpanjiang Basin (modified from Yan 2013). **C**, photograph of shark strata (Layers
 819 8-9, Yang et al., 1984) of Luolou Formation at ZD I section. **D**, photograph of shark strata (Layer
 820 11, Yang et al., 1984) of Luolou Formation at ZD II section. NB = Nanpanjiang Basin.



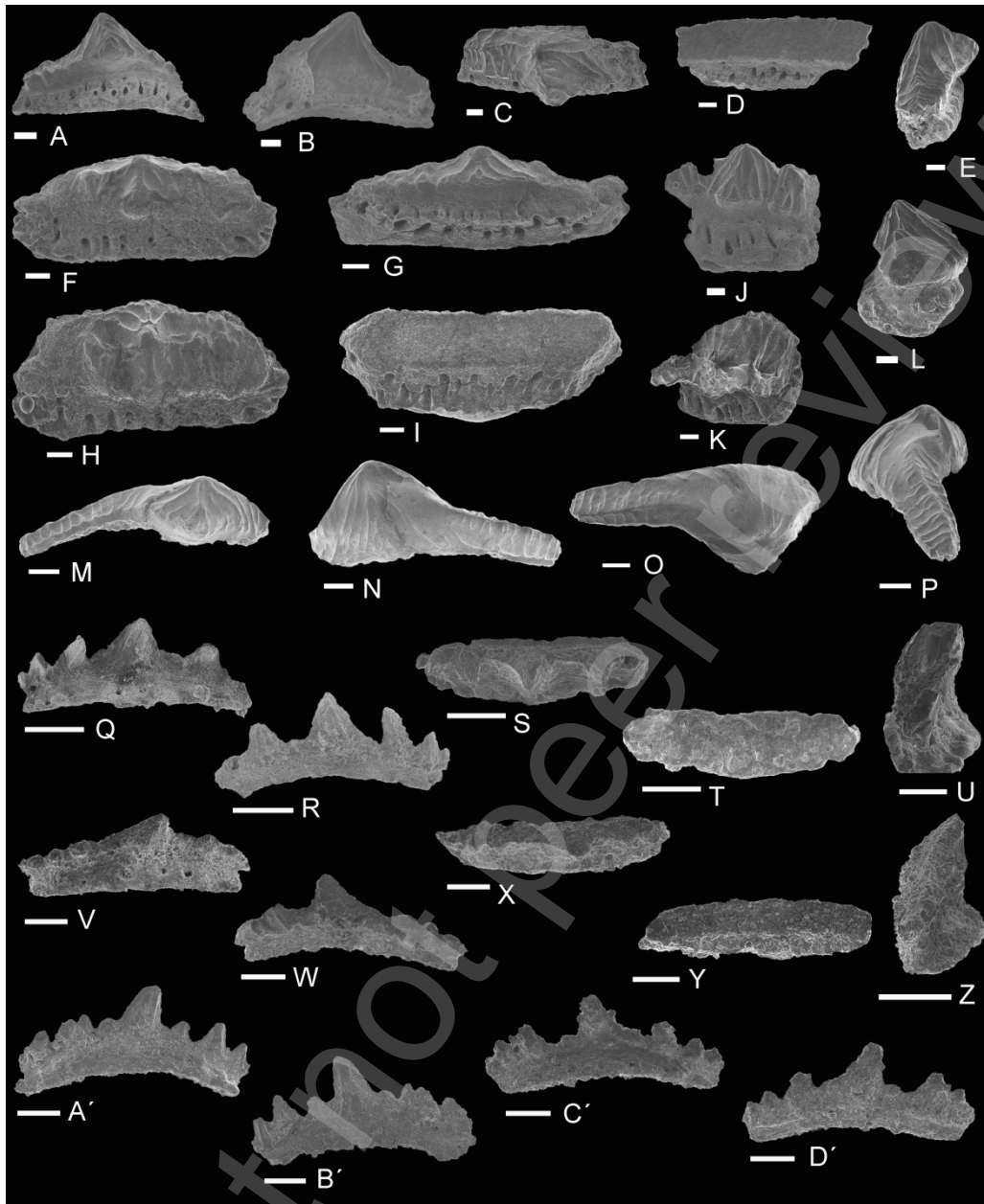
822 FIGURE 2. Stratigraphic distribution of the fossils recovered from the Smithian–Spathian
 823 boundary of the Zuodeng locality. **A**, the stratigraphic column re-drawn based on Wang et al.,
 824 2001; **B**, ZD I section, **C**, ZD II Section. (modified from Yan 2013). *N. dieneri* = *Neospathodus*
 825 *dieneri*, HM = *Hindeodus minutus*, HP = *Hindeodus parvus*, II = *Isarcicella isarcica*, NC
 826 = *Neospathodus cristagalli*, CC = *Clarkina carinata*, NW = *Novispathodus waageni*, *D. discreta* =
 827 *Discretella discreta*, *I. collinsoni* = *Icriospathodus collinsoni*, TH = *T. homeri* = *Triassospathodus*
 828 *homeri*, *N. waageni* = *Novispathodus waageni*, PP = *Pachycladina-Parachirognathus*, NP =
 829 *Novispathodus pingdingshanensis*. Ch = Changhsingian, He = Heshan.



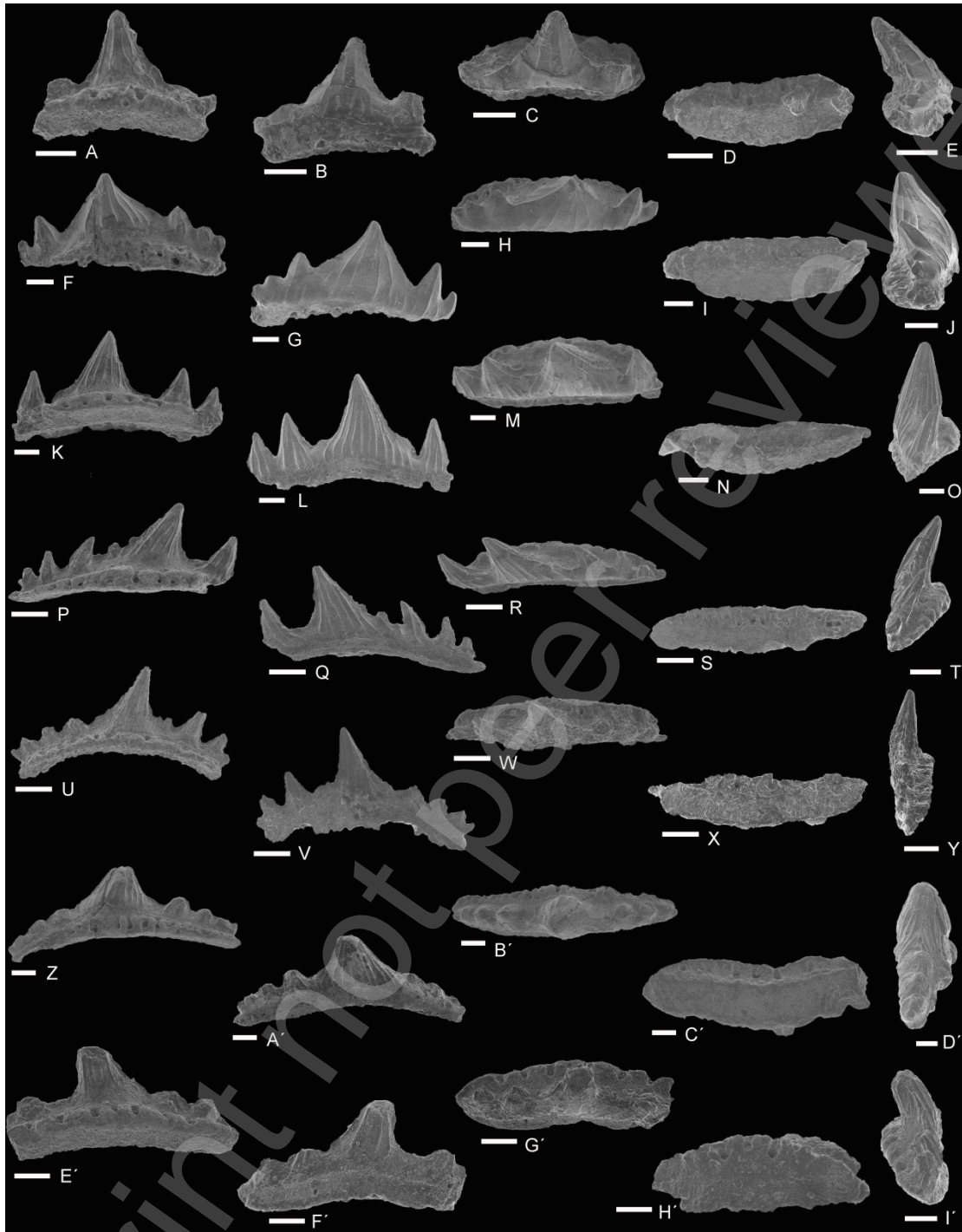
830 FIGURE 3. Teeth of *Omanoselache halli*. **A-E**, anterior tooth, GMPKU-P-3750; **F-J**, anterolateral
 831 tooth, GMPKU-P-3751; **K-O**, anterolateral tooth, GMPKU-P-3752; **P-T**, lateral tooth,
 832 GMPKU-P-3753; **U-Y**, posterior tooth, GMPKU-P-3754. **A, F, K, P** and **U** in lingual views; **B, G,**
 833 **L, Q** and **V** in labial views; **C, H, M, R** and **W** in apical views; **D, I, N, S** and **X** in basal views; **J**
 834 and **O** in mesio-apical views; **E** and **T** in disto-apical views; **Y** in mesio/disto-apical view. Scale
 835 bars equal 200 μm . Microstructure of the enameloid of *Omanoselache halli*. **Z**, GMPKU-P-3799,
 836 etched 5 seconds in 10% HCL, crystallites at crown surface. **A'-C'**, GMPKU-P-3790, **A'-B'**,
 837 etched 30 seconds in 10% HCL, crystallites of vertical ridges in **A'** and longitudinal crest in **B'**;
 838 **C'**, etched 30 seconds in 10% HCL, dentine of the lower part of the crown. Scale bars: **Z'-B'**,
 839 equal 2 μm ; **C'** equals 50 μm .



840 FIGURE 4. A-U. Teeth of *Hybodus* sp. A-E, GMPKU-P-3780; F-J, GMPKU-P-3781; K-O,
 841 GMPKU-P-3782; P-S, GMPKU-P-3783. A, F, K and P in lingual views; B, G, L and Q in labial
 842 views; C, H, M and R in apical views; D, I and N, in basal views; E, J, O and S in lateral views.
 843 Scale bars equal 200 μ m. Microstructure of the enameloid of *Hybodus* sp. T-U, GMPKU-P-3782.
 844 T, etched 15 seconds in 10% HCL, crystallites of cutting edge. U, etched 20 seconds in 10% HCL,
 845 crystallites of labial face on the apex. V-W. Microstructure of the enameloid of *Favusodus*
 846 *orientalis*. GMPKU-P-3775. V, etched 20 seconds in 10% HCL, enameloid of the longitudinal
 847 section of the crown. W, etched 25 seconds in 10% HCL, crystallites at the occlusal crown surface.
 848 Scale bars: T-U, W equal 2 μ m; V equals 20 μ m.

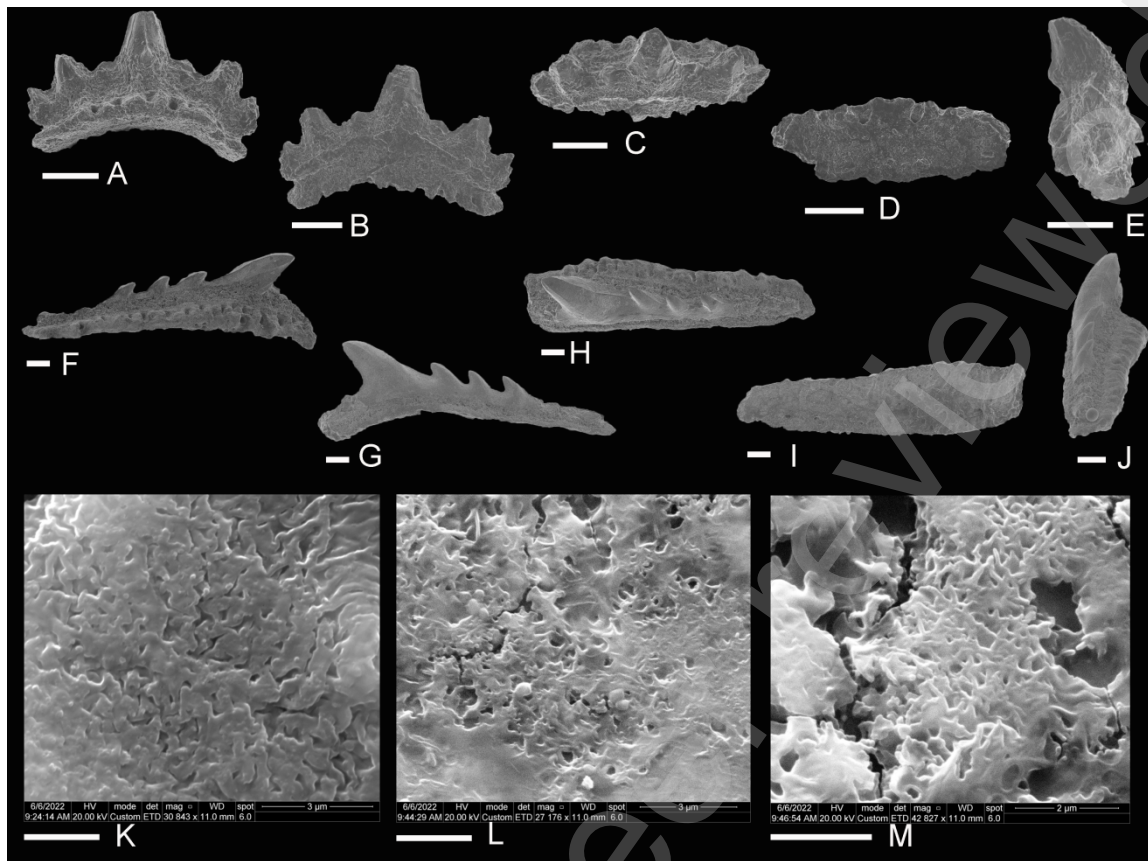


850 FIGURE 5. A-P. Teeth of *Favusodus orientalis*. A-E, GMPKU-P-3771; F-I, GMPKU-P-3772;
 851 J-L, GMPKU-P-3773; M-P, GMPKU-P-3774. Q-D'. Teeth of *Euselachii* gen. et sp. indet. Q-U,
 852 GMPKU-P-3777; V-Z, GMPKU-P-3778; A'-B', GMPKU-P-3779; C'-D', GMPKU-P-3792. A, F,
 853 J, M, Q, V, A' and C' in lingual views; B, G, N, R, W, B' and D' in labial views; C, K, H, O, S
 854 and X in apical views; D, I, T and Y in basal views; E, L and P in disto-apical views; U and Z in
 855 lateral views. All scale bars equal 200 μ m.

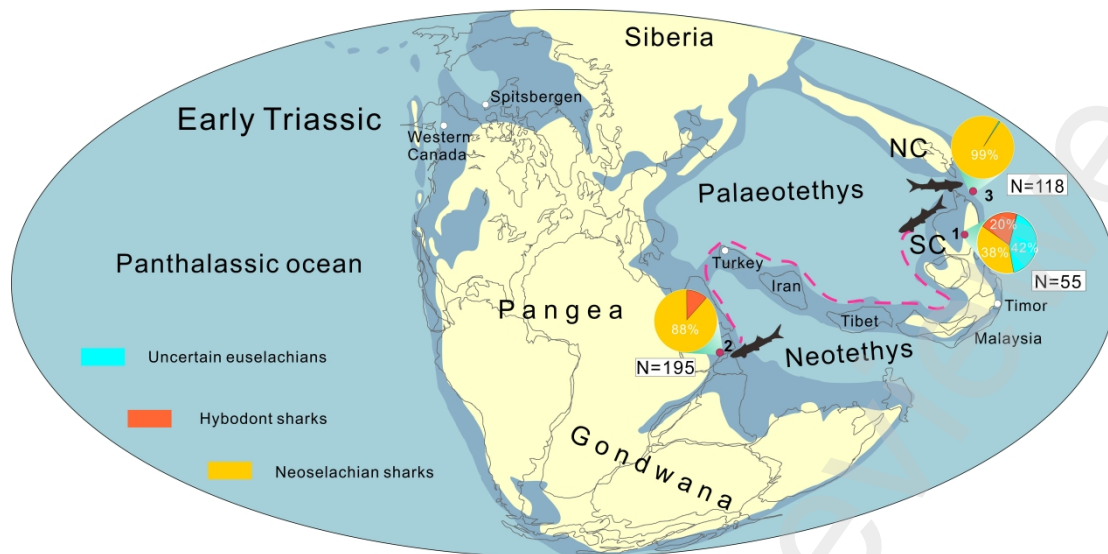


857

858 FIGURE 6. Teeth of *Safrodus tozeri*. **A-E**, anterior tooth, GMPKU-P-3762; **F-J**, anterolateral
 859 tooth, GMPKU-P-3763; **K-O**, lateral tooth, GMPKU-P-3764; **P-T**, lateral tooth, GMPKU-P-3765;
 860 **U-Y**, GMPKU-P-3766; **Z-D'**, posterolateral tooth, GMPKU-P-3767. **E'-I'**, posterolateral tooth,
 861 GMPKU-P-3768. **A, F, K, P, U, Z** and **E'** in lingual views; **B, G, L, Q, V, A'** and **F'** in labial
 862 views; **C, H, M, R, W, B'** and **G'** in apical views; **D, I, N, S, X, C'** and **H'** in basal views; **D'** in
 863 mesio-apical view; **E, J, O, T, Y** and **I'** in lateral views. All scale bars equal 200 μ m.



865 FIGURE 7. **A-E.** Tooth of *Polyfaciodus pandus*. anterolateral tooth, GMPKU-P-3770. **F-J.** Tooth
 866 of *Synechodus* aff. *triangulus*. GMPKU-P-3769. **K-M.** Microstructure of the enameloid of
 867 *Safrodus tozeri*. GMPKU-P-3762, etched 5 seconds in 10% HCL. **K**, crystallites at the apex of the
 868 main cusp; **L-M**, crystallites of the lower part of the crown. **A** and **F** in labial views; **B** and **G** in
 869 lingual views; **C** and **H** in apical views; **D** and **I** in basal views; **E** in mesio/disto-apical view; **J** in
 870 mesio-apical view. Scale bars: **A-J**, equal 200 μm ; **K-L**, equal 2 μm .



871 FIGURE 8. The palaeobiogeographic distribution and relative abundance of major groups of
 872 Chondrichthyes among western Neotethys and eastern Palaeotethys during the Early Triassic.
 873 Palaeogeographic maps modified from Scotese (2014) and Lyu et al., (2018). 1 represents
 874 Zuodeng; 2 represents Oman; 3 represents southwest Japan. N= the number of teeth in a given
 875 shark fauna. The red dash line represents the hypothetical migration route.